RSC Advances

PAPER

View Article Online
View Journal | View Issue

Cite this: *RSC Adv.*, 2025, **15**, 40823

Semi-interpenetrating polymer network ion-solvating membrane with enhanced conductivity and stability for potential application in alkaline water electrolysis

Mina Jellab, Loubna Ahsaini, Mustapha Matrouf, Fatima-Zahra Semlali * and Fouad Ghamouss*

This study presents a new semi-interpenetrating polymer network (semi-IPN) membrane, combining polyvinyl alcohol (PVA) cross-linked with citric acid (CA) and physically entangled with of polyvinylpyrrolidone (PVP) *via* solvent casting. To achieve a suitable balance between ionic conductivity, mechanical stability, and long-term chemical resistance, a series of PVA-CA:PVPX membranes were synthesized and subsequently subjected to thermal curing and KOH doping. Optimized PVP content stabilizes the semi-IPN structure by reinforcing H-bonding with PVA, resulting in a well-entangled polymer matrix. However, excessive PVP disrupts polymer chain interactions, leading to excessive microphase separation, extreme swelling, and diminished mechanical integrity. Thermal curing further strengthens crosslinking, enhancing mechanical properties (1270 MPa tensile modulus, 413% elongation) while controlling water uptake (193.96%). Additionally, KOH doping introduces carboxylate groups, increasing OH^- mobility (6.56 mS cm^{-1}) and improving electrochemical performance. The optimized membrane demonstrates high oxidative stability, retaining 90.90% of its mass after prolonged exposure while maintaining structural integrity over three months in alkaline conditions. Furthermore, its enhanced thermal stability extends operational lifespan under elevated temperatures, making it a promising candidate for long-term electrolysis applications. These findings establish semi-IPN structuring as an effective strategy for developing high-performance membranes suited for next-generation alkaline water electrolyzers.

Received 20th August 2025
Accepted 21st October 2025

DOI: 10.1039/d5ra06171g

rsc.li/rsc-advances

1 Introduction

The growing urgency to transition from fossil fuels to sustainable energy solutions has sparked global interest in hydrogen as an energy carrier.[1,2] Among the various production methods, water electrolysis is the most promising, especially when powered by renewable energy sources, due to its low capital cost and absence of greenhouse gas emissions.[1–3] Traditional alkaline water electrolysis (AWE) utilizes a porous diaphragm and a concentrated KOH solution (30–40 wt%). This enables the use of cost-effective, non-platinum-group metal catalysts, such as nickel foam, under alkaline conditions.[4] However, these electrolyzers operate with high cell voltages (1.7–2.4 V) and low current densities (300–400 mA cm^{-2}), resulting in low voltage efficiency and high internal resistance.[5] Additionally, carbonation of the KOH electrolyte can reduce durability by increasing ion-transport resistance and obstructing mass transport in gas diffusion layers.[6] Further challenges, such as gas permeation through the porous diaphragm and the risk of electrolyte blow-out, can negatively impact long-term performance and stability.[6]

To overcome these limitations, dense, non-porous polymeric membranes have been introduced to replace the porous separators. Proton exchange membranes (PEMs) and anion exchange membranes (AEMs) offer several advantages, including the production of high-purity hydrogen due to their superior gas barrier properties. The use of a thick membrane at high differential pressures enhances structural integrity, ensuring durability and long-term stability.[7] PEMs have been widely used in fuel cells and water electrolyzers. However, a major barrier to their large-scale commercialization is the high cost, primarily due to the membrane electrode assembly, which consists of a state-of-the-art Nafion membrane and expensive platinum-based catalysts.[8] Anion exchange membrane water electrolyzers (AEMWEs) have attracted significant attention due to their potential to combine the advantages of the AWE with the rapidly developing PEM water electrolysis.[9,10] Pt-free metal catalysts and inexpensive stack

Materials Science, Energy and Nanoengineering Department (MSN), Mohammed VI Polytechnic University (UM6P), Lot 660 – Hay Moulay Rachid, Ben Guerir, 43150, Morocco. E-mail: fatimazahra.semlali@um6p.ma; fouad.ghamouss@um6p.ma

hardware can be utilized in alkaline polymeric electrolytes, while low gas permeation is maintained. However, the low alkaline stability of AEMs (<5000 hours) and reduced durability at temperatures above 60 °C remain significant challenges.[11] Degradation caused by 2nd order nucleophilic substitution (SN2), Hofmann elimination of cationic groups, and free radical attack weakens both mechanical strength and conductivity, ultimately affecting long-term performance.[11] To bridge the gap in water electrolysis technologies, an operationally flexible polymer electrolyte membrane with strong ion conduction, high alkalinity, and stability at elevated temperatures (≥80 °C) is essential.

However, the presence of fixed cationic groups in polymer membranes can significantly limit their stability under AWE conditions.[4] Ion-solvating membranes (ISMs) are considered a promising alternative for producing green hydrogen in alkaline water electrolyzers. These combine the high efficiency and gas barrier properties of membrane electrolyzers with the advantages of conventional alkaline electrolyzers, such as ease of use and affordability.[12,13] When immersed in a KOH solution, ISMs facilitate hydroxide ion conduction by forming a homogeneous ternary electrolyte system consisting of polymer, KOH, and water.[12,13] Unlike porous diaphragms, ISMs are typically non-porous yet can be fabricated as thin as other polymeric membranes, achieving ionic conductivity through electrolyte uptake rather than intrinsic hydroxide conductivity. Typical ISMs are based on polybenzimidazole (PBI),[14] poly(ethylene oxide) (PEO),[15] and poly(vinyl alcohol) (PVA).[16,17] Xing *et al.*[14] demonstrated the feasibility of PBI-based ISMs for AWE, achieving a current density of 1.7 A cm^{-2} at 1.8 V using a Raney nickel catalyst. However, the electrochemical performance of PBI ISMs was highly dependent on alkaline absorption, and their long-term stability remained a concern due to hydroxide-induced degradation at the imidazole C2 position, leading to polymer chain scission.[6,13] To address this limitation, Diaz *et al.*[18] developed hybrid ISMs by blending PBI with PVA, leveraging PVA's hydrophilicity to enhance ion transport while maintaining mechanical integrity. Further stabilization was achieved through glutaraldehyde (GA) crosslinking, which improved long-term performance in alkaline conditions.

Among various polymeric candidates, PVA has gained attention for its strong alkali resistance and high hydrophilicity.[19,20] It has been successfully utilized as an electrolyte material in zinc-air batteries and is considered a promising structural backbone for ISMs. Additionally, PVA has been studied as an ion-solvating membrane due to its ability to absorb and retain aqueous alkaline electrolytes, enabling hydroxide ion conduction.[19,20] Lewandowski *et al.*[17] showed that optimizing the composition of PVA-KOH-H_2O membranes resulted in conductivity levels approaching 10^{-3} S cm^{-1}, with electrochemical stability ranging from 1.5 V to 2.75 V depending on the electrode material. Similarly, Palacios *et al.*[16] demonstrated that PVA-based alkaline solid electrolyte membranes, when combined with KOH and water, achieved a conductivity of up to 2.3×10^{-3} S cm^{-1} at room temperature, with further enhancement under higher humidity due to the plasticizing effect of water.

However, despite its promising properties, pristine PVA suffers from excessive swelling and limited mechanical stability in alkaline environments, which restricts its long-term use in water electrolysis. Notably, cross-linked PVA-based semi-IPN membranes have demonstrated enhanced properties. Amnuaypanich *et al.*[21] reported that semi-IPN structures based on PVA effectively reduced excessive swelling while maintaining water absorption. Similarly, Qiao *et al.*[22] developed a PVA-based semi-IPN membrane cross-linked with GA and incorporated PVP for AEM applications. However, GA-based crosslinking presents safety and stability concerns, necessitating alternative crosslinking strategies.[23]

Overall, the development of hydroxyl-conducting membranes aims to minimize energy losses while maintaining high conductivity, gas barrier properties, and mechanical strength. Achieving a balance between conductivity and tensile strength is challenging, as increasing ion-exchange capacity (IEC) enhances conductivity but also leads to excessive swelling, compromising membrane integrity. While crosslinking and reinforcement improve mechanical strength, they often reduce conductivity.[24] Semi-IPN membranes overcome this limitation by incorporating a stable polymer network that enhances ion transport, controls swelling, and ensures durability, all while preserving optimal electrochemical performance.[25]

To the best of our knowledge, no previous study has reported the development of a semi-IPN ISM based on PVA cross-linked with citric acid and combined with PVP, nor has any investigation focused on optimizing PVP concentration, assessing the effect of thermal treatment, or exploring KOH doping in such systems. In this study, semi-IPN ISMs composed of PVA, citric acid, and PVP were fabricated using the solvent-casting method. Following synthesis, the membranes underwent thermal treatment and were immersed in KOH solution to introduce specific properties. The primary objective was to evaluate how increasing PVP content and its physical entanglement influence the formation of the semi-IPN structure and to determine the optimal PVP concentration. Furthermore, the effects of thermal treatment and KOH doping on the membrane's physicochemical and electrochemical properties were investigated. By examining these key parameters, this study offers valuable insights into the interplay between material composition, structural optimization, and post-treatment strategies, contributing to the advancement of ISMs for potential application in water electrolysis.

2 Materials and methods

2.1 Materials

Poly(vinyl alcohol) (PVA) (average Mw 130 000, 99+% hydrolyzed), polyvinylpyrrolidone (PVP) (average Mw = 40 000), and citric acid (CA) monohydrate ACS reagent (≥99.5%) were purchased from Sigma-Aldrich Co. Ltd and used without further treatment. All chemical products used in this study, including potassium hydroxide (KOH), silver nitrate ($AgNO_3$) (99.8–100.5%), sodium sulfate (Na_2SO_4) (≥99%), hydrogen peroxide (30%) (H_2O_2), iron(II) sulfate ($FeSO_4$) (≥99%), and potassium dichromate (K_2CrO_4) were supplied by Sigma-Aldrich. All

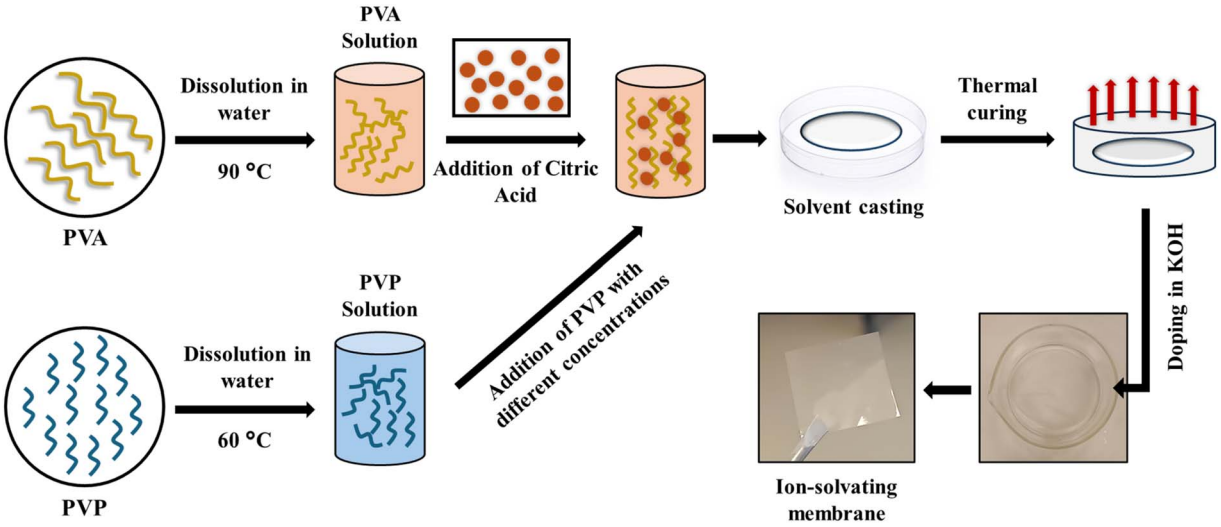

Fig. 1 Schematic of the ion-solvating membranes fabrication process.

reagents were of analytical grade and used without further purification. All solutions in this study were prepared with distilled water (pH = 5, conductivity of 14.79 μS cm^{-1})

2.2 Membrane preparation

All the ISMs were prepared using the solvent casting technique (Fig. 1). Initially, 10 g of PVA were dissolved in 100 mL of distilled water at 90 °C for 6 hours, and 10 g of PVP were dissolved in 100 mL of distilled water at 60 °C for 3 hours, to obtain clear and homogeneous solutions. Subsequently, 20% citric acid was introduced into the PVA solution and stirred for 2 h at 60 °C to initiate the crosslinking reaction. To investigate the potential effects of PVP on the membrane properties, the prepared PVP solution was then added to the cooled PVA-CA mixture. Thus, solutions comprising different concentrations of PVA-CA and PVP were prepared (PVA-CA:PVPX) in the following ratios: 1 : 0, 1 : 0.25, 1 : 0.5, 1 : 0.75, 1 : 1, and 1 : 1.5. These mixtures were stirred continuously at 60 °C for 3 h to ensure uniform mixing and poured into Petri dishes at room temperature. After complete solvent evaporation, the resulting membranes underwent thermal treatment at 130 °C for 1 h to continue the cross-linking process.

To impart anion conductivity, the membranes were immersed in a 3 M KOH solution for 3 h at 60 °C to enhance the hydroxide ion transfer capacity. They were then thoroughly washed with distilled water to remove excess KOH. The resulting ISMs included the neat PVA membrane as the reference, while the others were denoted as PVA-CA:PVPX, where X refers to the PVP ratio (X = 0, 0.25, 0.5, 0.75, 1, 1.5).

3 Characterization techniques

3.1 Fourier transform infrared spectroscopy (FTIR)

The chemical structure of the membranes was characterized using Fourier transform infrared spectroscopy (FTIR, PerkinElmer Spectrum 2000, Waltham, Massachusetts, United State). This analysis was conducted in the range of 600–4000 cm^{-1}, using 32 scans per spectrum and a 4 cm^{-1} spectrum resolution.

3.2 Soxhlet extraction

This procedure was conducted to assess the structural stability and resistance of the membranes in an aqueous environment. The dried membrane was placed in a Soxhlet apparatus, and the extraction was carried out using water at 100 °C for 24 hours. This process aimed to evaluate the membrane's ability to retain its components under prolonged exposure to water.[26] After extraction, the membrane was thoroughly dried to eliminate any residual moisture, ensuring accurate mass measurements. The membrane mass was measured before (W_i) and after extraction (W_f) to evaluate the mass change.

The weight retention was calculated as follows:

$$R(\%) = \frac{W_f}{W_i} \times 100 \quad (1)$$

3.3 Scanning electron microscopy (SEM)

The top and cryofractured cross-section views of the developed membranes were examined using a scanning electron microscope (SEM, ZEISS EVO 10, GmbH, Jena, Germany) at an operating voltage of 10 kV. To avoid electrical charging during imaging, the samples were coated with a layer of gold sputtering (5 kV accelerated voltage) in an ionization chamber beforehand.

3.4 Water uptake and swelling ratio

The measurements of the membranes' water uptake (WU) and swelling ratio (SR) were conducted by assessing the membrane's changes in mass and dimension after immersing them in water. Initially, the membranes underwent drying in an oven at 60 °C for 24 hours to determine the dry weight (W_{dry}) and the dry state (L_{dry}). Subsequently, the membranes were soaked in deionized water for 24 hours. The excess of water was removed from the

surface, and the membranes were weighed to determine the wet weight (W_{wet}) and measured to determine the wet length (L_{wet}). The WU and SR of the membranes were calculated as follows:

$$WU = \frac{W_{wet} - W_{dry}}{W_{dry}} \times 100 \quad (2)$$

$$SR = \frac{L_{wet} - L_{dry}}{L_{dry}} \times 100 \quad (3)$$

3.5 Alkaline stability

To assess the alkaline stability of the ISMs, they were initially immersed in a 1 M KOH solution at room temperature for 48 hours. The mass of the membranes was measured before and after the alkaline stability test. Additionally, images of the membranes were captured both before and after immersion to visually inspect any structural or morphological changes. For long-term stability evaluation, the selected membranes were submerged in the same 1 M KOH solution for three months, thoroughly rinsed with deionized water, and analyzed using FTIR spectroscopy to assess any changes in their chemical composition. To further approximate real alkaline electrolysis conditions, membranes were tested for one week in 1 M KOH at 60 °C, followed by mass retention measurements and FTIR analysis to assess structural stability.

3.6 Oxidative stability

To evaluate the oxidative stability of the membranes under harsh oxidative conditions, the membranes were exposed to Fenton reagent treatment (3% H_2O_2 with 3 ppm $FeSO_4$) for 8 h at 60 °C. Following exposure, the membranes underwent a 2 h drying process at 60 °C after being rinsed with deionized water, and their post-treatment dry weight was determined. To assess their resistance to oxidative degradation, changes in weight and physical characteristics, such as discoloration or brittleness, were compared to pre-treatment conditions. Understanding the membranes' durability in oxidative environments depends on this analysis.

3.7 Ion exchange capacity (IEC)

The Mohr method was utilized to determine the IEC value of the membrane and assess its concentration of interchangeable ionic groups. After measuring the dried membrane samples, they were directly immersed for 24 h in an aqueous solution of 1 M NaCl, which converted the ion exchange groups to Cl^- ions. The samples were then removed from the solution and gently rinsed with deionized water. They were then immersed in an aqueous solution containing 0.5 M Na_2SO_4 for 48 h to substitute Cl^- ions with SO_4^{2-} ions. An aqueous solution of K_2CrO_4 was used as an indicator, and titration with a 0.05 M aqueous solution of $AgNO_3$ was used to calculate the amount of substituted Cl^- ions.

The following formula was used to determine IEC:

$$IEC = \frac{C_{AgNO_3} V_{AgNO_3}}{W_{dry}} \quad (4)$$

where C represents the concentration of $AgNO_3$, V the volume of $AgNO_3$ and W_{dry} is the weight of the dried membrane sample.

3.8 Hydroxide conductivity

Hydroxide conductivity was measured using electrochemical impedance spectroscopy (EIS) in a zero-gap configuration. The membrane was sandwiched between two stainless steel electrodes using a 1 M KOH electrolyte at room temperature. Impedance measurements were conducted over a frequency range of 200 kHz to 100 MHz with an AC voltage amplitude of 10 mV.[27,28] The membrane resistance (R) was determined from the impedance measurements, and hydroxide ion conductivity (σ, ms cm^{-1}) was calculated using the following equation:

$$\sigma = \frac{L}{A \times R} \quad (5)$$

where L is the distance between the two electrodes or the thickness of the membrane, A is the active area, and R is the resistance attributed to the membrane.

3.9 Thermogravimetric analysis (TGA)

The thermal stability of the prepared membranes was assessed using a thermogravimetric analyzer apparatus (Discovery TGA, TA instruments New Castle, United State). The tests were performed under a nitrogen atmosphere (25 mL min^{-1}) at a heating rate of 10 °C min^{-1} from 25 °C to 900 °C.

3.10 Tensile test

Tensile tests were performed at room temperature using a Universal Testing Machine Texture Analyzer (SHIMADZ, Kyoto, Japan) with a gauge length of 30 mm, a crosshead speed of 5 mm min^{-1}, and a 1 kN load cell in accordance with ISO 527-5. The produced membranes were therefore trimmed into a rectangle shape (10 × 50 mm^2), and the representative value was stated as the average of five specimens.

4 Results and discussion

4.1 Manufacturing process and mechanisms

This study presents a novel approach to designing high-performance ISMs with improved ionic conductivity and structural stability for electrochemical applications. This approach combines PVA, citric acid, and PVP to develop robust semi-IPN membranes with tailored physicochemical properties. Different PVA-based membrane formulations were synthesized, thermally cured, and alkali-doped to maximize mechanical strength, electrochemical durability, and ionic transport capabilities.

To ensure structural integrity, efficient crosslinking, and uniform polymer dispersion, a series of critical steps were implemented in the production process. PVA was first dissolved in deionized water under controlled heating and continuous stirring to promote polymer chain relaxation and homogeneity. The crosslinking reaction was subsequently initiated by the carefully controlled addition of citric acid, which formed ester bond with the PVA's hydroxyl groups. This reaction was

necessary to decrease solubility, strengthen intermolecular connections, and increase resistance to dissolution in aqueous environments, thereby improving the membrane's thermal, mechanical, and chemical durability.[29]

To further improve flexibility and ionic conductivity, PVP, acting as both a plasticizer and structure modifier, was incorporated at different concentrations. The role of PVP extends beyond improving mechanical properties, as it also promotes the formation of semi-IPN structures through physical entanglement within the cross-linked PVA network.[30–32] This interaction directly affects the morphology, porosity, and ion transport properties of the membrane.[33] The purpose of optimizing PVP concentration is not only to establish a balance between mechanical stability and ion mobility, but also to identify the transition point at which the material develops into a stable semi-IPN structure.[27,29] The proposed mechanism of semi-IPN formation is illustrated in Fig. 2, highlighting how PVP chains physically entangle within the cross-linked PVA matrix. The objective of this study is to determine the threshold concentration at which PVP entanglement occurs without destroying the cross-linked PVA matrix, ensuring the coexistence of the cross-linked and the physically interpenetrating polymer phases.

At low PVP concentrations, the network remains largely governed by cross-linked PVA, resulting in a rigid structure with limited flexibility and restricted ion transport pathways.[29] Conversely, excessive PVP concentration increases the mobility of the polymer chains, thereby weakening the mechanical integrity of the membrane and reducing its structural durability under operating conditions.[34,35] Therefore, accurately determining the PVP concentration for semi-IPN formation is important to maintain mechanical robustness and maximize the interconnectivity of ion transport pathways.[34,35] In addition, the hydrophilicity of PVP affects the membrane's ability to absorb water and plays an important role in maintaining high ionic conductivity.[30–32] Controlled increases in PVP content can promote water absorption, thereby improving hydration of ion charge carriers and reducing interface resistance. However, excessive water absorption can lead to swelling and potential structural degradation during long-term use.[30–32] By fine-tuning the PVP ratio, water absorption can be precisely controlled to ensure optimal hydration levels without compromising mechanical integrity.

To systematically evaluate these effects, a series of membrane formulations were prepared with different PVA-CA to PVP ratios (1 : 0, 1 : 0.25, 1 : 0.5, 1 : 0.75, 1 : 1, and 1 : 1.5), transitioning from a PVA-rich to a PVP-rich matrix. This gradual change in PVP content allows for a thorough examination of its impact on membrane characteristics, making it easier to determine the ideal composition that targets the precise conditions for semi-IPN formation while achieving the optimal balance between mechanical strength, ionic conductivity, and electrochemical stability.

In addition to compositional optimization, heat treatment and alkaline doping are important factors in defining the final membrane properties. In order to strengthen the crosslinking between PVA and citric acid and stabilize the semi-IPN network, the membranes in this investigation were thermally cured at 130 °C. The hydroxyl groups of PVA and citric acid form ester bonds when heated to this temperature, improving the material's mechanical strength, chemical resistance, and structural integrity.[22,36] The removal of leftover solvents by this heat treatment also results in a denser, defect-free membrane structure. Heating also helps with phase separation between PVA and PVP, which can affect porosity and, in turn, the ionic transport behavior of the membrane.[22,36]

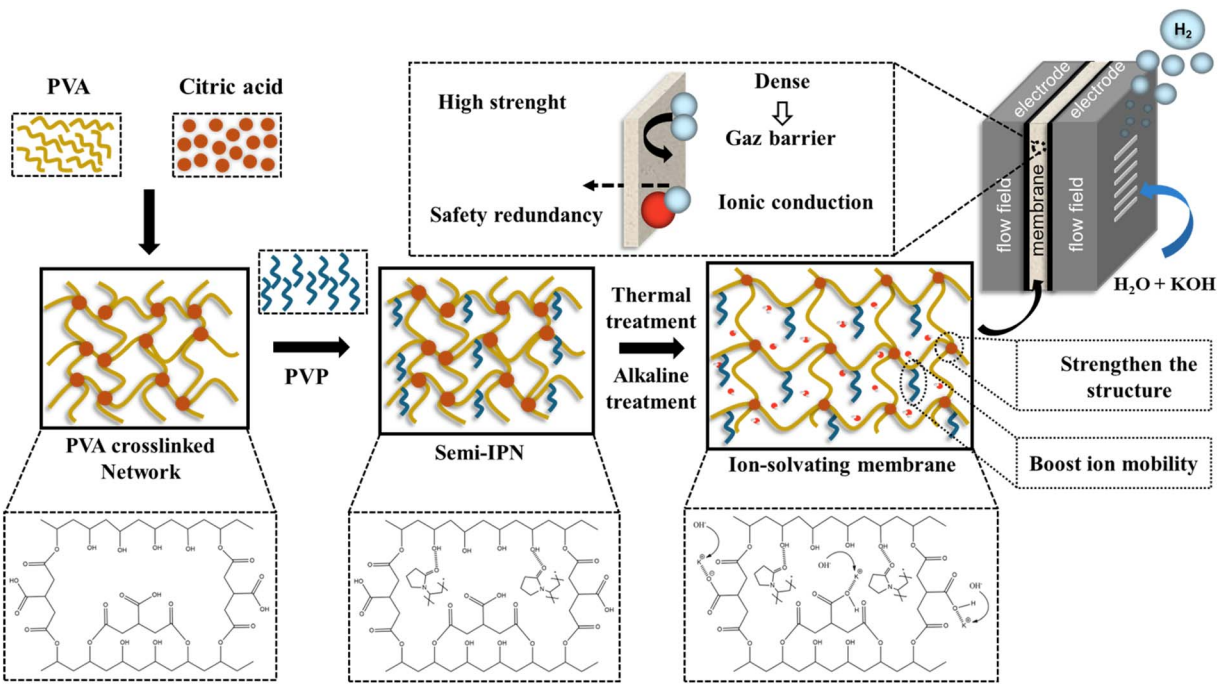

Fig. 2 Manufacturing process and mechanisms of the elaborated ion-solvating membranes.

After heat treatment, the membranes were doped with KOH solution. This process is commonly referred to as "cooking".[33,37] This alkali treatment is essential to convert the membrane into an ion-solvating structure suitable for electrochemical applications.[33,37] The KOH treatment partially hydrolyzes the free carboxylic acids of the citric acid, forming negatively charged functional groups that facilitate ion exchange and improve ion conductivity. In addition, the interaction of KOH with the polymer matrix increases the hydrophilicity of the membrane, improving water retention and promoting the efficiency of ion transport pathways.[33,37] Controlling swelling through the addition of KOH also helps to maintain sufficient mechanical robustness to withstand operating conditions while modulating membrane flexibility and ensuring that ion transport is not hindered.[33,37]

This study offers important insights into the interaction between polymer composition, crosslinking mechanisms, and post-processing alterations by methodically examining the impacts of PVP concentration, thermal treatment, and alkaline doping. With potential uses in water electrolysis and other electrochemical energy conversion systems, these discoveries further the development of ISMs. These findings contribute to the advancement of ISMs with potential applications in water electrolysis and other electrochemical energy conversion systems.

4.2 Chemical structural analysis

The membranes after thermal treatment were subjected to FTIR spectroscopy both before and after KOH doping to gain a better understanding of the ion solvation process and its structural evolution. This analysis provides information on the chemical interactions causing the membrane to change into an ion-solvating system and enables the identification of functional group changes. Fig. 3a presents the FTIR spectrum of the neat PVA membrane before cooking in KOH, revealing a broad absorption band in the 3200–3400 cm^{-1} range, which corresponds to the hydroxyl groups of PVA, confirming hydrophilicity and strong hydrogen bonding.[38] The two distinct bands observed at 2912 and 2942 cm^{-1} correspond to symmetric and asymmetric stretching vibrations of methylene (-CH_2) groups in the PVA backbone.[39] The band observed at 1659 cm^{-1} is associated with bending vibrations of hydroxyl groups, indicating the presence of a large number of free hydroxyl groups.[39] The polymer's aliphatic structure is confirmed by the band at 1421 cm^{-1}, which is linked to the bending vibration mode of methylene (–CH_2) groups.[40] Meanwhile, the peak at 1329 cm^{-1} is associated with bending vibrations of hydroxyl groups (δ(OH)) and vibrations of methylene groups (CH wagging).[40] The crystalline portion of PVA exhibits stretching vibrations of C–O bonds in the band at 1145 cm^{-1}, while the amorphous sections of PVA exhibit bending vibrations of hydroxyl groups and stretching vibrations of C–O bonds in the band at 1085 cm^{-1}.[40] The CH_2 and C–C stretching vibrations in the PVA polymer chain are represented by the other peaks at 917 cm^{-1} and 848 cm^{-1}, respectively.[40]

When PVA was cross-linked with citric acid, significant changes appeared in the FTIR spectrum, indicating successful chemical alterations. Upon crosslinking with citric acid, an ester linkage is formed between the hydroxyl group of PVA and the carboxyl group of citric acid.[33] This is confirmed by the appearance or enhancement of a new peak around 1710–1740 cm^{-1} corresponding to stretching vibrations of the ester carbonyl group (C=O).[33] The broad absorption band in the range 3200–3400 cm^{-1} is related to the hydroxyl group and may be slightly shifted with decreasing intensity due to depletion of the hydroxyl group during esterification or changes in the hydrogen bonding network.[33] The interaction between the hydroxyl groups of PVA and citric acid is further confirmed by the decreased intensity of the band at 1659 cm^{-1}, which is associated with the bending vibrations of free hydroxyl groups.[33] Changes in the local chemical environment brought on by crosslinking may also produce slight variations in the peak at 1421 cm^{-1}, which is linked to the scissoring and wagging of methylene (–CH_2) groups.[33] Additionally, the amorphous region's peak at 1085 cm^{-1} and the crystalline region's peak at 1145 cm^{-1} showed variations in the band intensity, indicating the structural reorganization of PVA upon crosslinking.[33,40]

Conversely, the lactam structure and functional groups of PVP are reflected in its characteristic FTIR bands (Fig. 3a). The lactam ring's carbonyl (C=O) stretching vibration, which is sensitive to hydrogen bonding and interactions with other components, is represented by the most noticeable peak, which arises at 1650 cm^{-1}.[33,41] The amide functionality is further confirmed by the appearance of the C–N stretching vibration at 1280 cm^{-1}.[37] The symmetric and asymmetric C–H stretching of the CH_2 groups in the aliphatic backbone is shown by peaks about 2800–3000 cm^{-1}, whilst the CH_2 groups exhibit bending and wagging motions around 1400–1500 cm^{-1}.[37,42] The 600–1100 cm^{-1} range is where vibrations linked to the cyclic lactam structure and C–C/C–O bonds are detected.[37]

Notable alterations in the FTIR spectra show the structural and chemical changes in the polymer matrix as the PVP content rises in relation to PVA and eventually exceeds it (Fig. 3b). The lactam ring's carbonyl (C=O) stretching vibration, the most noticeable characteristic linked to PVP, is usually seen between 1650 and 1665 cm^{-1} and grows more and more pronounced as the PVP content increases.[33,41,43] This suggests that PVP is becoming more prevalent in the composite system. Increased hydrogen bonding interactions between PVP's carbonyl groups and the remaining PVA hydroxyl groups or the remaining citric acid carboxyl groups may potentially contribute to this peak's increased intensity. The broad O–H stretching band around 3200–3400 cm^{-1}, which characterizes the PVA hydroxyl groups and their associated hydrogen bonding network, change further with increasing PVP content.[38] The intensity of this band decrease and the band shape broaden as PVP amide groups form hydrogen bonds with PVP and citric acid components, disrupting the original PVP hydrogen bonding network.[38]

Other PVP-specific peaks, such as C–N stretching vibrations in the 1290–1350 cm^{-1} region, become more prominent with increasing PVP concentration, further confirming their increasing contribution to the overall chemical structure.[37] Similarly, the intensity of aliphatic C–H stretching vibrations in the 2800–3000 cm^{-1} region and CH_2 bending vibrations and

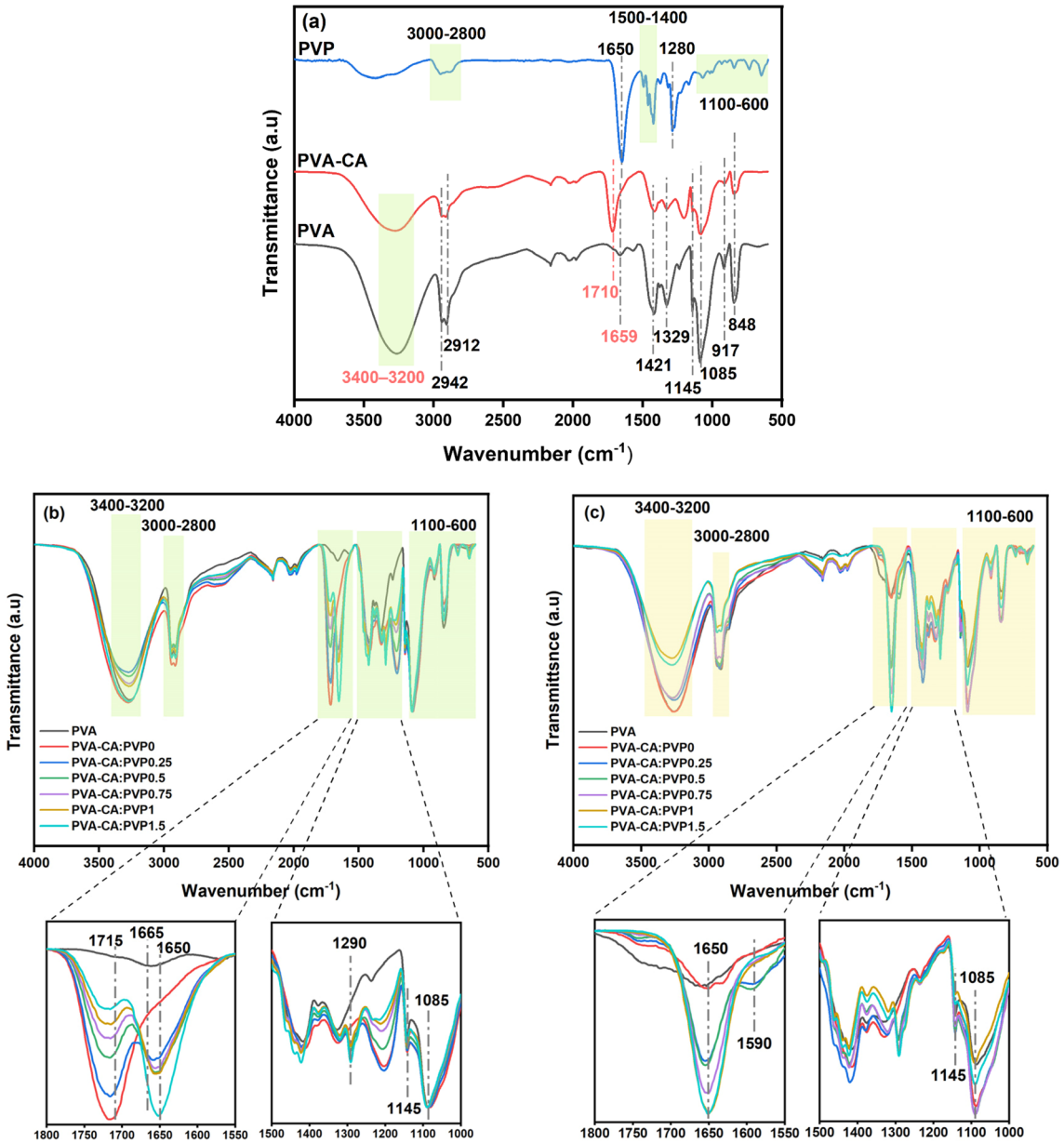

Fig. 3 FTIR spectra of (a) PVP, PVA, and cross-linked-PVA, (b) the prepared membranes before KOH doping, (c) the prepared membranes after KOH doping.

vibrational motions in the 1400–1500 cm^{-1} region also increase with increasing the proportion of PVP in the matrix.[37,42,44] The vibrations associated with the cyclic lactam structure and C–C/C–O bonding of PVP are more pronounced in the lower wavelength range (corresponding to 600–1100 cm^{-1}).[37] The peaks at 1085 cm^{-1} (C–O stretching of amorphous PVA) and 1145 cm^{-1} (C–O stretching of crystalline PVA) may be slightly shifted or attenuated in intensity as the proportion of PVA in the matrix decreases and its crystalline and amorphous structure is destroyed by PVP.[37,42,45]

These spectral shifts show how PVP is incorporated into the PVA-citric acid matrix and provide insight into how PVP, PVA, and citric acid interact chemically as PVP content rises. Significant effects on the physical and chemical characteristics of the resultant membranes are caused by the dominance of PVP-related peaks when its concentration exceeds PVA, which confirms the shift to a PVP-rich matrix.

Following cooking in KOH (Fig. 3c), the FTIR spectra shows notable spectral shifts, indicating structural and chemical changes in the polymer matrix. The intensity of the broad absorption band corresponding to the hydroxyl group (–OH) in the range 3200–3400 cm^{-1} may be altered or shifted due to the partial hydrolysis of ester bonds, leading to the formation of additional hydroxyl groups that increase the hydrophilicity of the membrane.[38] The partial ester bond hydrolysis was further confirmed by the appearance of new carboxylate ($–COO^-$) bands at 1550–1600 cm^{-1} and by the decreased intensity of the ester carbonyl (C═O) stretching band at 1710–1740 cm^{-1}.[33]

PVP's C=O stretching vibration, which occurs between 1650 and 1665 cm^{-1}, exhibits peak broadening or intensity fluctuations as a result of novel hydrogen bonding interactions with carboxylate and hydroxyl groups.[33,41] Disruption of PVA crystalline domains and increased amorphization, which promotes ion transport, are shown by the weakening or shifting of the bands at 1085 cm^{-1} (C–O stretching of amorphous PVA) and 1145 cm^{-1} (C–O stretching of crystalline PVA).[37,42] Following KOH treatment, the polymer chain's flexibility may cause bending vibrations in the 1400–1500 cm^{-1} range to shift, while the symmetric and asymmetric stretching vibrations of methylene ($-CH_2$) groups in the 2800–3000 cm^{-1} region may slightly lessen in intensity.[37,42]

Furthermore, higher intensity in the 600–1100 cm^{-1} area indicates improved ion solvation interactions brought on by the new ionic species creation and the inclusion of K^+ ions.[46] As a result of these changes, the polymer matrix is reorganized, carboxylate groups are formed, and ester bonds are partially hydrolyzed, improving flexibility, water absorption, and ionic conductivity. The membrane is more appropriate for electrochemical applications, including water electrolyzers, due to the diminution of PVA crystalline peaks and the appearance of larger ionic interaction bands, which further suggest a shift toward a more amorphous, ion-solvating structure.

4.3 Soxhlet extraction test

When evaluating the structural integrity and chemical stability of ISMs, the Soxhlet extraction test is essential. It provides insight into the degree of crosslinking, the solubility of membrane constituents, and the compatibility of the polymers within the matrix.[47] In this study, to confirm the formation of the semi-IPN and further assess the stability and structural integrity of the prepared membranes, a Soxhlet extraction was performed using water as the solvent. Water was selected for its ability to dissolve the primary components of the membranes, PVA,[48] PVP,[49] and citric acid,[50] and to simulate real operating conditions, offering insight into the membrane's resistance to aqueous environments. Water also allows for a more comprehensive evaluation of the network's cohesion by testing the solubility and leaching behavior of PVA, PVP, and citric acid. This approach helps determine the effectiveness of crosslinking, the retention of polymeric constituents, and the overall durability of the membrane in practical applications.[47]

As shown in Fig. 4, the Soxhlet extraction test demonstrates that the alkali-treated PVA membrane exhibits strong resistance to dissolution, with a retention rate of 98.32%. This high retention is attributed to the presence of robust hydrogen bonds between polymer chains, which prevent excessive dissolution during the extraction process.[51] Additionally, thermal and alkali treatments further enhance PVA's resistance to dissolution. Thermal treatment stabilizes the material by increasing its degree of crystallinity through the alignment of polymer chains.[52–54] Meanwhile, alkali treatment induces partial deacetylation, reinforcing the polymer structure while slightly reducing its solubility.[55]

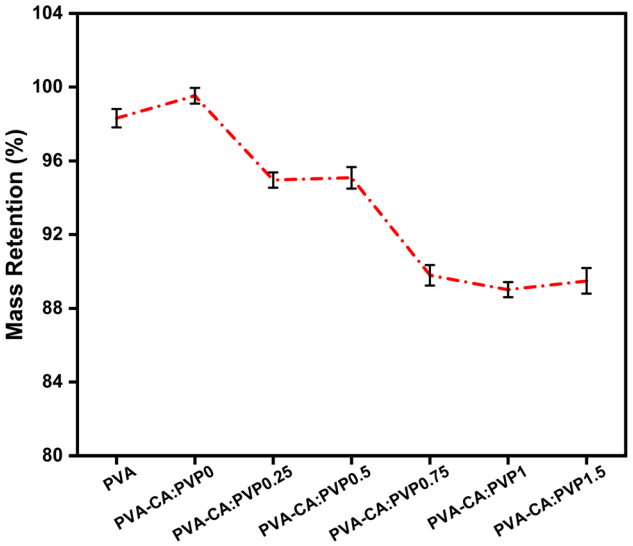

Fig. 4 Mass Retention of the prepared ion-solvating membrane during Soxhlet extraction.

For the PVA-CA:PVP0 membrane, retention increased to 99.53%, demonstrating that citric acid crosslinking enhances membrane stability. The slight improvement compared to neat PVA suggests that the cross-linked network effectively restricts the leaching of polymeric components, further confirming the successful formation of a stable polymer structure. The high retention confirms that citric acid effectively crosslinks PVA through esterification reactions, enhancing the membrane's chemical resistance while preserving its structural integrity. The optimal amount of citric acid, 20 wt%, used in this work, is the ideal ratio for crosslinking PVA membranes.[56] This is supported by several studies,[57] including S. M. Huang *et al.*'s findings,[56] which demonstrate that 20% citric acid improves membrane performance and stability.

In PVA-CA:PVP0.25 and PVA-CA:PVP0.5 membranes, retention remains close to 95%, although slightly lower than in the fully cross-linked PVA-CA membrane. This slight decrease in retention indicates that the introduction of a sufficient amount of PVP does not significantly compromise the cohesion of the polymer matrix. At these concentrations of PVP, the chains are physically entangled in the cross-linked PVA-CA network, forming a semi-IPN. This structure allows PVP to confer useful properties, such as increased flexibility and hydrophilicity, without disturbing the integrity of the chemically cross-linked domains.[30–32] The ester bonds formed between citric acid and PVA continue to maintain the membrane backbone and prevent large-scale dissolution even after prolonged exposure to boiling water. Hydrophilic groups added from the PVP may contribute to a small amount of water absorption and cause a slight weight loss, but the overall network remains very dense and robust.[30–32] At this stage, no significant leaching occurs because of the large PVP domains and low integration. Thus, the membrane retains both physical integrity and functional potential, indicating that semi-IPN structures with controlled PVP content can be an

effective compromise between structural stability and desired performance.[33]

As the PVP content increases (PVA-CA:PVP0.75, PVA-CA:PVP1, and PVA-CA:PVP1.5), retention declines more significantly to 89.79%, 89.02%, and 89.49%, respectively. At greater concentrations, the PVP-rich phase dominates, resulting in a softer, more flexible, and water-absorbent membrane. Water stability is reduced, even though this may improve ionic conductivity and ion transport. The main causes of decreased retention are increased solubilization of PVP chains, reduced intermolecular interactions within the matrix, and possibly insufficient entanglement or integration of PVP into the PVA-CA network.[31,34,35] The network is further altered by the KOH treatment, which partially hydrolyzes ester bonds and introduces carboxylate groups to impart anion conductivity. This approach, especially in PVP-rich conditions, might increase water swelling and membrane hydrophilicity, resulting in more material loss during Soxhlet extraction.[33]

Overall, Soxhlet extraction with water confirms that crosslinking enhances membrane stability while excessive PVP incorporation compromises structural cohesion. These findings highlight the need to optimize polymer composition to achieve a balance between stability, ionic conductivity, and long-term durability in electrochemical applications.

4.4 Morphological observations

The thermally treated and KOH-conditioned membranes' morphological evolution (Fig. 5) shows clear structural changes as the formulations' composition changes from PVA-rich to PVP-rich, highlighting how phase behavior, crosslinking, and polymer interactions affect membrane architecture and shape their potential as ISMs. Pure PVA and PVA-CA have a dense and cohesive surface, which is indicative of robust intermolecular interactions and ester crosslinking that reinforce the membrane's structural integrity and minimize irregularities.[58] Small additions of PVP (PVA-CA:PVP0.25 and PVA-CA:PVP0.5) result in a perceptible increase in porosity and heterogeneity of the membrane surface, according to SEM images. This suggests that PVP, which is only introduced by physical entanglement, modifies the compact arrangement of the cross-linked network.[30–32] This results in regions where the polymer chains are not as tightly packed, resulting in microvoids and textural differences that are also visible on the cross-section. Based on these features, a semi-interpenetrating matrix is formed, in which the PVP domains expand and create a more open structure, while the cross-linked PVA-CA component preserves a core backbone, which is in good agreement with Soxhlet results.[30–32] However, with further increases in PVP content (PVA-CA:PVP0.75 and PVA-CA:PVP1.5), the morphology shifts once again, returning to a denser, more homogeneous appearance. In membranes with higher PVP content, the interactions between the PVP chains become more pronounced, creating areas of cohesive polymer entanglement that lessen the apparent porosity, thus reducing the extent of phase separation.[31,34,35] The cross-sectional views support this pattern, demonstrating that membranes with higher PVP ratios regain a cohesive network with fewer noticeable voids, whereas those with intermediate PVP levels have a rougher, more irregular internal structure.

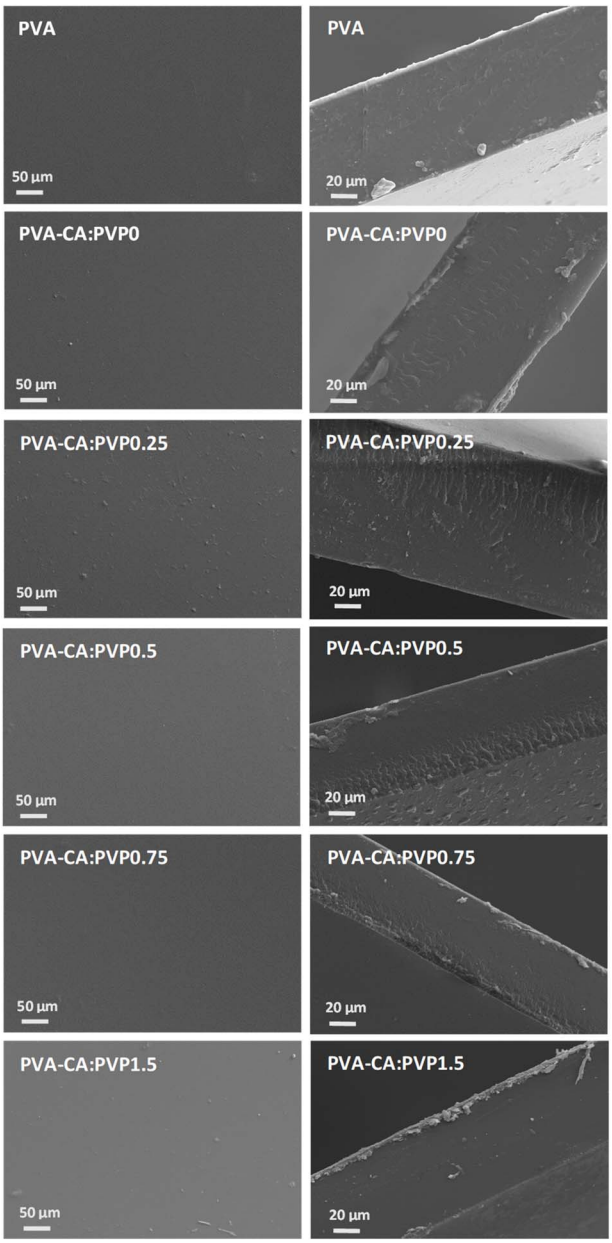

Fig. 5 Top and cross-sectional views of the prepared ion-solvating membranes.

These results imply that moderate PVP concentrations (0.25–0.5), where the interaction between porosity, free volume, and polymer cohesion is well tuned, may be the ideal balance for ion-solvating applications. At these compositions, the membrane structure maintains mechanical stability to avoid excessive swelling or deterioration while remaining open enough to allow efficient ion transport. PVP-rich membranes, on the other hand, may show decreased ionic mobility because of polymer densification, whereas PVA-rich membranes, despite their structural strength, may restrict ion diffusion because of

their compact nature. In order to produce ISMs that balance hydration, dimensional stability, and effective ion conduction for electrochemical applications such as alkaline electrolyzers, it is imperative to accurately manage the polymer composition and phase distribution.

4.5 Water uptake and swelling ratio

Water absorption and swelling are critical to the performance of ISMs as they directly affect ion transport, mechanical integrity and structural stability under operating conditions.[36,59] High water absorption ensures sufficient hydration of functional groups for efficient hydroxide ion transport, while controlled swelling prevents deformation and damage to the structure.[59] The structural alterations brought about by thermal treatment at 130 °C and subsequent immersion in KOH, as well as the molecular interactions generated during synthesis, are strongly related to the variations in water absorption and swelling seen across various membrane compositions. These post-processing treatments are essential for improving crosslinking, preserving polymer connections, and altering the network of polymers' hydrophilic-hydrophobic balance.[31,34,35]

Fig. 6 shows that the water absorption and swelling of the produced membranes vary in three different regions, each reflecting different structural interactions and modifications. In the first region, from pure PVA to PVA-CA:PVP0 and PVA-CA:PVP0.25, the water absorption increases significantly from 60.09% for pure PVA to 193.96% for PVA-CA:PVP0.25, indicating the progressive enhancement of membrane hydrophilicity. Neat PVA's high hydroxyl groups, which have a strong interaction with water molecules, contribute to its roughly 60.09% water absorption.[33] Nevertheless, significant swelling compromises dimensional stability when crosslinking is absent.[33] Citric acid crosslinking introduces ester linkages, creating a stiff three-dimensional network that restricts the mobility of polymer chains. The distinctive esterification peaks of FTIR analysis demonstrate that this stabilization decreases swelling while preserving a moderate increase in water absorption (157.87%). Modest hydrophilicity and decreased swelling are caused by alkali treatment in KOH, which also strengthens network rigidity by promoting additional crosslinking reactions and boosting residual carboxyl functionalities.[33,37] When PVP is added to the cross-linked PVA-CA matrix, its hydrophilic lactam groups (C=O) significantly enhance water absorption. Water uptake increases significantly at 0.25% PVP, reflecting the enhanced hydrophilicity of the system. This may support the creation of a stable semi-IPN, where the physically entangled PVP chains enhance hydrophilicity and contribute to water uptake, while the cross-linked PVA-CA structure provides mechanical strength.[30–32] SEM images provide further evidence of this result, showing that the addition of 0.25 wt% PVP results in the formation of a more porous structure, enabling greater water absorption. PVP's lactam carbonyl groups form a strong hydrogen bond with the hydroxyl and carboxylic groups of PVA-CA, allowing PVP to be integrated into the cross-linked matrix.[30,31] As observed in FTIR spectra, thermal treatment also strengthens these interactions by promoting chemical rearrangement and stronger hydrogen bonds. In order to prevent excessive swelling and improve water uptake, the semi-IPN arrangement achieves a balance between water retention and structural integrity.[30,31] Tests of Soxhlet extraction confirm the system's stability and reveal extremely low weight loss, demonstrating that the cross-linked PVA-CA network efficiently holds onto PVP and inhibits leaching.

In the second region, from PVA-CA:PVP0.25 to PVA-CA:PVP0.75, both water absorption and swelling decrease. As the cross-linked matrix approached the saturation point of retained PVP, water absorption decreased from 193.96% to 136.93%. Excess PVP disrupted the network homogeneity, reduced the density of semi-IPNs, formed PVP-rich micro-regions, limited water penetration and reduced swelling.[34,35] Soxhlet results in this region show a slight weight loss due to leaching of some of the poorly integrated PVP, but the semi-IPN remains relatively stable. Furthermore, thermal treatment stabilizes the network against excessive expansion by strengthening hydrogen bonds and enhancing polymer packing, which further reduces swelling. Similarly, KOH doping alters the ionic environment of the polymer by adding negatively charged carboxylate ($-COO^-$) groups, which repel excess hydration over a certain threshold and reduce excessive water uptake.[30,31]

In the third region from PVA-CA:PVP0.75 to PVA-CA:PVP1.5, the water absorption of PVA-CA:PVP1.5 increases again to 210.76%, but the swelling shows a more complex pattern. Initially swelling decreases as the network becomes denser and less flexible, as confirmed by SEM analysis, which reveals a densely packed structure. Notwithstanding the dense SEM appearance, swelling develops once again at PVA-CA:PVP1.5 because of the presence of extra PVP molecules that are not yet completely incorporated into the cross-linked matrix. This effect is explained by the development of hydrophilic PVP-rich microdomains, which absorb a lot of water while also decreasing structural stability by causing internal tensions from excessive swelling.[31,34,35] Soxhlet extraction results in this area

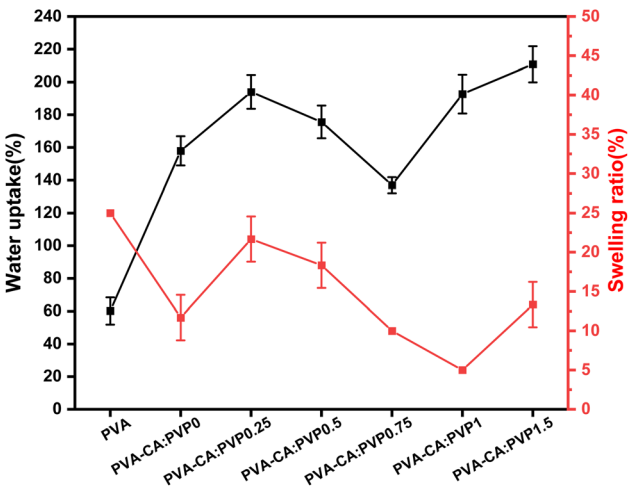

Fig. 6 The water uptake and swelling ratios of the prepared membranes.

show significant weight loss, which confirms the leaching of unbound PVP and the instability of the semi-IPN structure.

These results highlight the need to carefully regulate PVP concentration, degree of cross-linking and post-processing treatments to maximize water uptake and swelling behavior. Controlling the hydrophilic-hydrophobic balance, strengthening the polymer network, and preventing excessive swelling while maintaining adequate hydration for ion transport are all made possible by thermal curing and KOH doping. The results demonstrate the need for precise compositional optimization to create high-performance ion-transport membranes that combine effective hydration, dimensional stability, and mechanical resilience.[31,34,35]

4.6 Alkaline stability

In alkaline water electrolyzers, the alkaline stability of ISMs is a key determinant of their long-term performance and durability. Prolonged exposure to strongly alkaline environments can lead to structural degradation, excessive swelling, and chemical instability, ultimately compromising membrane integrity and efficiency.[60] Ensuring high alkaline stability is therefore crucial for sustained operation and long-term applicability in electrochemical systems.[61] The alkaline stability test of the prepared membranes was conducted under three conditions: (i) immersion in 1 M KOH at room temperature for 48 h, (ii) immersion in 1 M KOH at room temperature for three months, and (iii) immersion in 1 M KOH at 60 °C for 1 week to simulate real operating conditions. Comparative assessment of resistance to alkaline degradation was made possible by monitoring structural and chemical changes using FTIR spectroscopy, mass retention, and visual inspection.

Short-term alkaline stability results show that most of the membranes tested show good stability in alkaline environments after 48 hours of immersion (Fig. 7). Both pure PVA and PVA-CA:PVP0 membranes retain 100% of their weight, consistent with strong retention during Soxhlet extraction. This stability is due to the thermal treatment at 130 °C for 1 h, which increases the crystallinity, strengthens hydrogen bonding, and creates a dense, rigid network, as confirmed by SEM images.[62] Cross-linking PVA with citric acid further produces a stable chemical structure that is resistant to both water solubilization and alkaline degradation.[52–55] Visual inspection of pre- and post-treatment images of these membranes shows little change in texture and structure, reflecting a robust network. The membranes appear smooth and dense before treatment and retain this integrity after treatment, showing no significant swelling or surface damage (Fig. 8a).

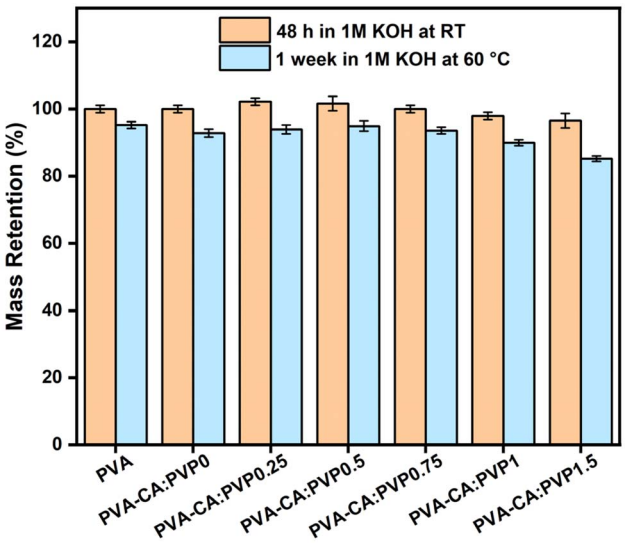

Fig. 7 Mass retention of the produced ISMs after 48 hours in 1 M KOH at room temperature and after 1 week in 1 M KOH at 60 °C.

For membranes with moderate concentrations of PVP (PVA-CA:PVP0.25 and PVA-CA:PVP0.5), the slight increase in mass retention during short-term alkalinity tests can be attributed to moderate swelling, as also suggested by the results of Soxhlet analysis (Fig. 4). The semi-IPN structure of these membranes, formed by physically weaving PVP into a cross-linked PVA-CA network, can control water uptake without significantly reducing stability.[63] The slight increase in retained mass (102.16% and 101.63%) indicates that the membranes absorb KOH solution, which does not significantly degrade the structure and can even improve electrochemical performance.[12,13,17] Following treatment, images of these membranes reveal a small whitening, most likely as a result of the increased hydrophilic PVP content, which interacts with the alkaline environment to produce moderate surface alterations. This slight color shift is a result of structural changes that are taking place without significant leaching or deterioration (Fig. 8a).

As PVP content increases, the relationship between the short-term alkalinity test and Soxhlet data becomes clearer: membranes with higher PVP concentrations (PVA-CA:PVP0.75, PVA-CA:PVP1 and PVA-CA:PVP1.5) showed reduced retention in both scenarios (Fig. 7). In the short-term alkalinity test, retention dropped to 97.9% and 96.53%, while the Soxhlet results showed a significant decrease in retention at similar PVP levels. This pattern underscores that high PVP content weakens overall network integrity. The flexibility and hydrophilicity added by PVP leads to greater susceptibility to leaching and degradation in both prolonged water exposure (Soxhlet) and alkaline environments.[31,34,35] When PVP content increases from 0.25 to 0.75, the membrane becomes even whiter, showing increased hydrophilicity and water absorption. However, at PVP1 and PVP1.5 contents, the films turn from white to transparent, indicating that the PVP-rich network phase dominates and alters the material's optical properties. This transparency may be the result of structural reorganization and reduced network density of PVA-CA, corresponding to poorer retention and reduced stability (Fig. 8a).

Furthermore, FTIR spectra after 48 hours of alkali treatment showed minimal changes (Fig. 9a). The broad band at 3200–3400 cm^{-1} associated with hydroxyl (–OH) stretching remained strong, indicating that the hydrogen bonds necessary for ion mobility had been preserved, while methylene ($–CH_2$) stretching peaks at 2920 and 2940 cm^{-1} confirmed the stability of the PVA backbone.[38] The peak at 1653 cm^{-1}, attributed to the

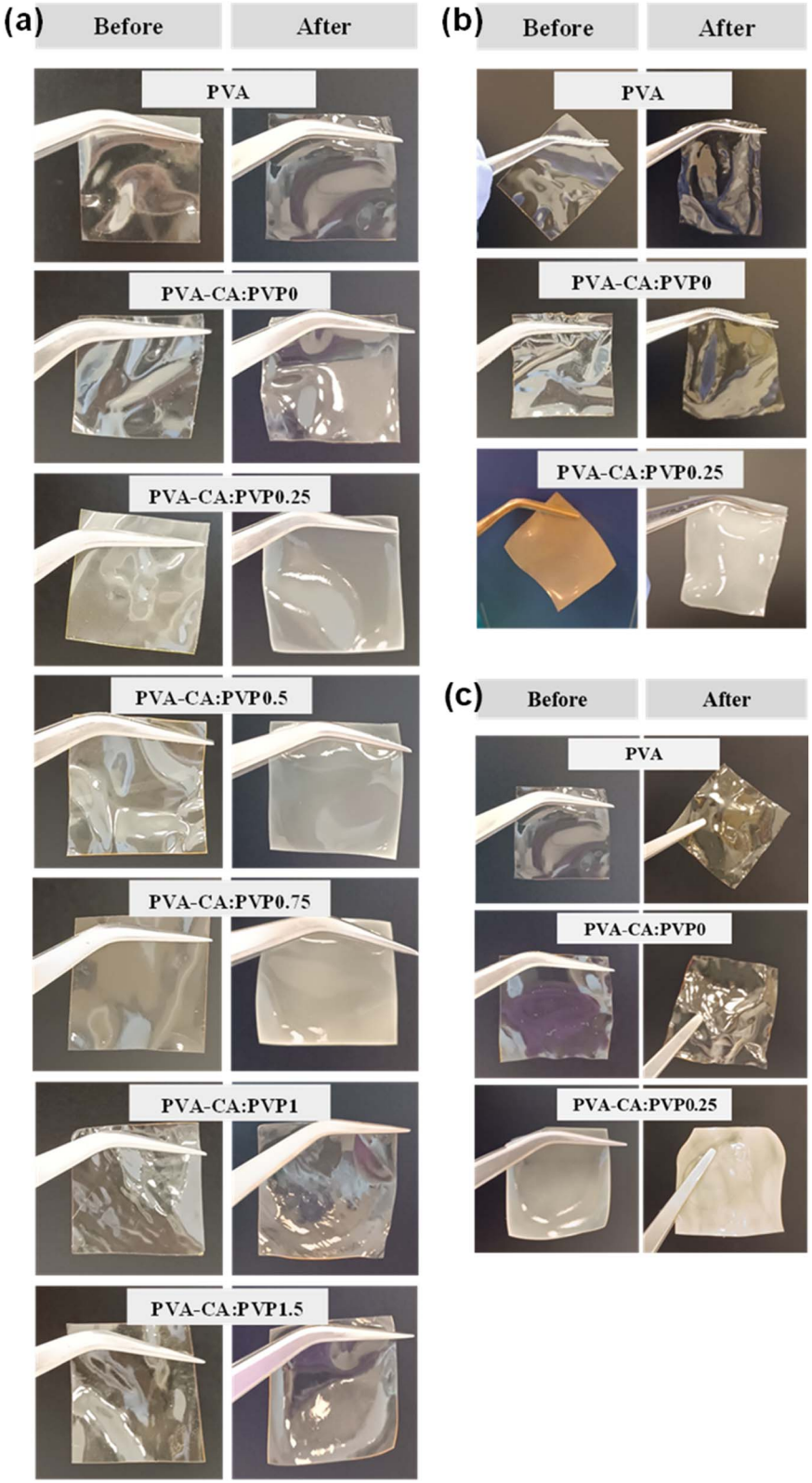

Fig. 8 Photographic comparison of ISMs before and after immersion in 1 M KOH for (a) 48 hours at room temperature, (b) 3 months at room temperature and (c) 1 week at 60 °C.

carboxylate groups ($-COO^-$) formed during the partial hydrolysis of the ester bonds, is still maintained, indicating the continued presence of citric acid crosslinking and contributing to enhanced alkali uptake and ionic conductivity.[33] In addition, the characteristic C–N stretching vibrations of PVP (1290–1350 cm^{-1}) are still visible, suggesting that PVP remains well

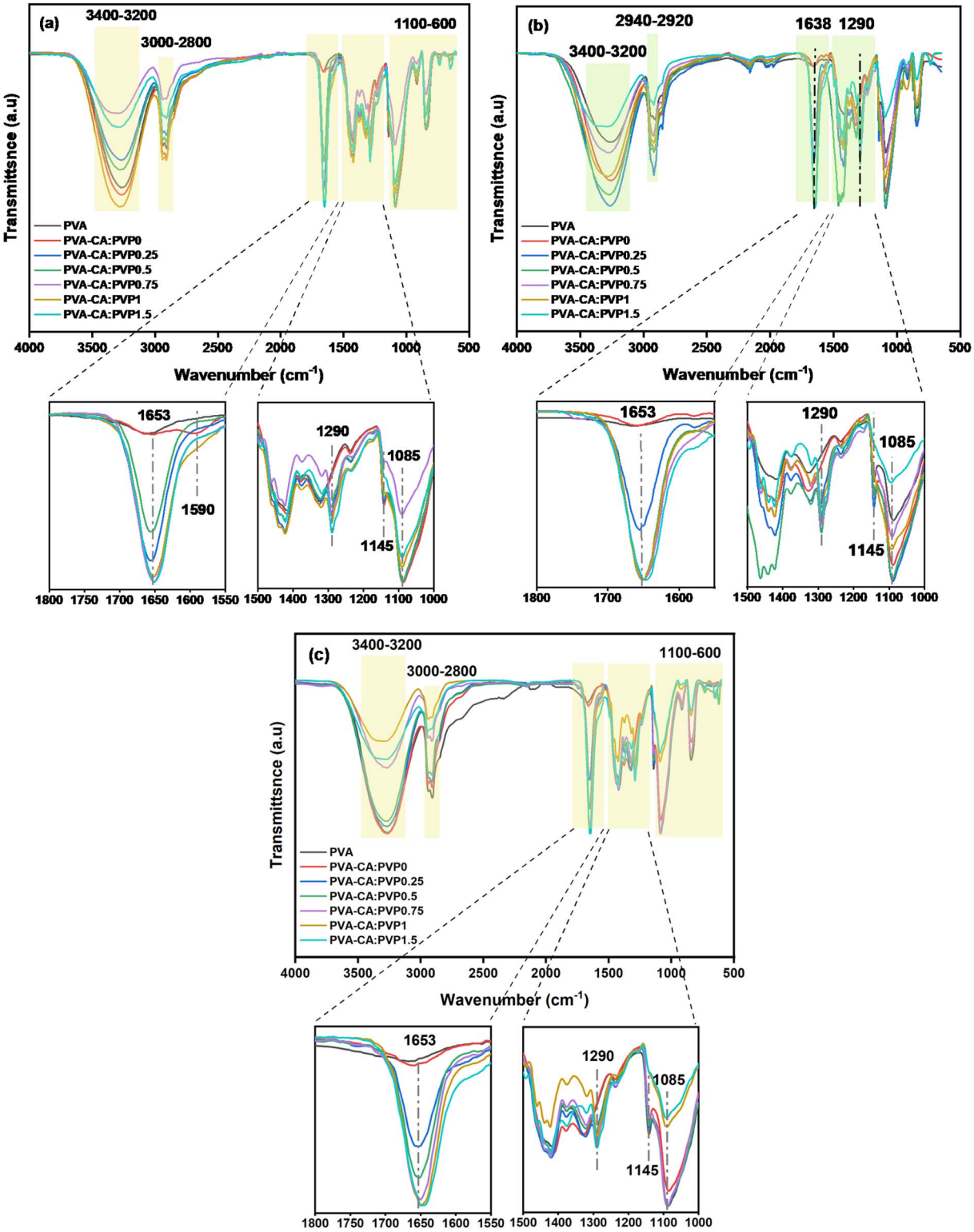

Fig. 9 FTIR analysis of the prepared membranes after immersion in 1 M KOH for (a) 48 hours at room temperature, (b) 3 months at room temperature and (c) 1 week at 60 °C.

embedded within the polymer matrix, preventing polymer leaching and maintaining the semi-IPN structure.[37]

After three months in 1 M KOH, the FTIR spectra showed more prominent bands with minor chemical changes (Fig. 9b). The presence of carboxylate groups, arising from the partial hydrolysis of ester linkages and the conversion of citric acid –COOH groups into their carboxylate form, was evidenced by the band at 1653 cm^{-1}.[30] It is generally recognized that this

modification increases the fixed charge density, which may improve ion conduction.[22] However, a slight reduction in the intensity of crystalline (1145 cm^{-1}) and amorphous (1085 cm^{-1}) PVA bands suggests minor changes in the polymer's morphology, potentially enhancing flexibility and facilitating ion transport.[37,42]

Following three months of alkaline exposure, morphological changes were visually assessed for three typical membranes: pure PVA, PVA-CA, and PVA-CA:PVP0.25 (Fig. 8b) to supplement FTIR results. At first, the pure PVA membrane appears smooth and transparent, but after three months in KOH, it wrinkles and becomes translucent, indicating disintegration due to excessive swelling. Similarly, when exposed to KOH, the PVA-CA membrane develops roughness and partial opacity, indicating a partial break in cross-linking caused by ester bond hydrolysis, as confirmed by the FTIR results. On the other hand, even after prolonged alkaline exposure, the PVA-CA:PVP0.25 membrane remains more stable and cohesive. There was no visible tearing, dissolving, or wrinkling in the membrane's structure. The most noticeable change was the color shift to white, which is attributed to enhanced hydration and the growth of PVP-rich domains. This stability is primarily tuned by the covalent ester cross-linked between PVA and citric acid, which provide chemically robust linkages, along with physical interpenetration of PVP linear chains that stabilize the structure. These mechanisms maintain mechanical integrity, prevent polymer dissolution, and enable long-term stability.[31,34,35]

To approximate real alkaline water electrolyzer conditions, membranes were immersed in 1 M KOH at 60 °C for one week (Fig. 7). Pristine PVA and PVA-CA-PVP0 membranes retained more than 92% of their initial weight, due to the thermal treatment and citric acid cross-linking.[52–55,62] Membranes with moderate PVP contents (PVA-CA:PVP0.25 and PVA-CA:PVP0.5) exhibited the highest mass retention values (>93%), consistent with the stabilizing role of balanced PVP entanglement.[30–32] By contrast, membranes with higher PVP loadings (≥1) showed lower retention (85–90%), reflecting the tendency of excessive hydrophilicity introduced by abundant PVP, which weakens the network stability. These results are fully consistent with the Soxhlet extraction results, where high PVP contents also correlated with reduced stability.[31,34,35] Visual inspection of the prepared membranes before and after immersion (Fig. 8c) presents further confirmation of their alkaline stability at elevated temperature. After one week, both pristine PVA and PVA-CA:PVP0 membranes retain their transparency and structural integrity, displaying only minor surface wrinkling. This highlights the importance of the network thermal treatment and crosslinking in preventing alkaline induced dissolution. In contrast, the membrane PVA-CA:PVP0.25 showed a minor whitening and slight surface roughness after immersion, which is due to distributed PVP domains. These domains enhance the water uptake and ion mobility without compromising the overall cohesion of the membrane. The absence of cracks, damage or delamination confirms that the semi-IPN architecture preserves mechanical stability even under accelerated alkaline and thermal exposure. FTIR analysis (Fig. 9c) of the prepared membranes after alkaline exposure at 60 °C confirmed the preservation of the key functional groups, including hydroxyl stretching at 3200–3400 cm^{-1},[38] methylene stretching vibrations of PVA backbone (2912 and 2942 cm^{-1}),[39] and carboxylate bands (1653 cm^{-1}). The characteristic C–N stretching vibrations of PVP (1290–1350 cm^{-1}) were also retained, demonstrating that PVP remained embedded in the polymer matrix, thereby, avoiding polymer leaching and maintaining the semi-IPN structure.[37]

These findings demonstrate that the semi-IPN based membranes maintain their chemical integrity and structural stability during both short- and long-term alkaline exposure, as well as at elevated temperatures. Overall, the combination of citric acid crosslinking and moderate PVP entanglement provides a balance between hydrophilicity and mechanical integrity, enabling resistance to alkaline degradation under the tested conditions and indicating their potential suitability for alkaline electrolysis environments.

4.7 Oxidative stability

ISMs oxidative stability is a crucial characteristic since, in applications like alkaline water electrolyzers, they are subjected to severe oxidative conditions and must sustain their structural integrity and ion-conducting capabilities over time.[64,65] Fig. 10 shows that the pristine PVA membrane has the highest oxidation resistance (98.92%). This is due to the chemical and structural changes induced by thermal and alkaline treatment.[65] Indeed, KOH treatment removes weak polymer chains, improves homogeneity and strengthens intra- and intermolecular hydrogen bonds in the polymer matrix.[29,66] By preventing reactive species like hydroxyl radicals produced by the Fenton reagent from penetrating, this procedure produces a dense, tightly packed structure that resists oxidative destruction.[66] This is further confirmed by the low weight loss observed in Soxhlet extraction tests demonstrating the strength and chemical stability of the alkali-treated PVA membrane.[66] These properties

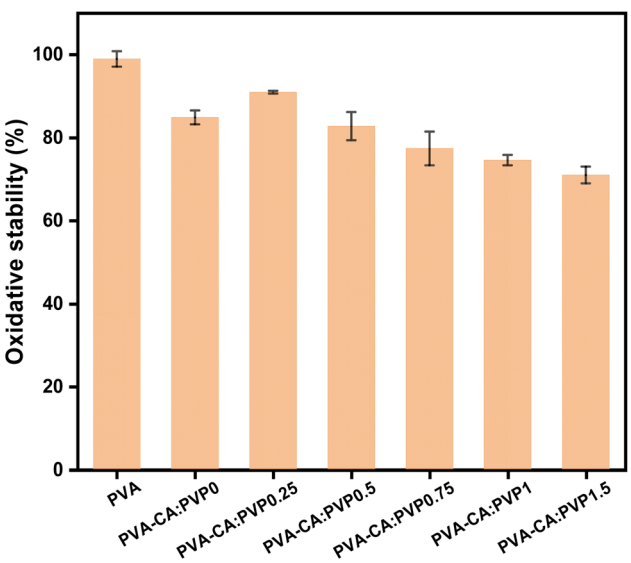

Fig. 10 Oxidative Stability of the ion-solvating membranes.

collectively provide the highest oxidative stability among all membranes.

Oxidative stability drops to 80.87% for cross-linked PVA-CA. By introducing ester bonds at the expense of hydroxyl groups, crosslinking lessens the polymer's ability to withstand oxidative degradation.[67] Under severe oxidative conditions, the polymer matrix is marginally more fragile because ester bonds are more susceptible to hydrolytic and oxidative attack.[22] The cross-linked structure also decreases flexibility, making the membrane more brittle and susceptible to oxidation over time, even if it increases dimensional stability and decreases swelling.[22,67] However, PVA-CA's reduced swelling as compared to pure PVA lessens the diffusion of reactive species, which helps prevent deterioration and almost offsets its sensitivity.[22,67]

When PVP is added at a low concentration (PVA-CA:PVP0.25), oxidative stability increases considerably to 90.9%, demonstrating the stabilizing effect of the semi-IPN that is formed at this stage. The advantages of cross-linked PVA-CA are combined with the hydrophilic and functional qualities of PVP in the semi-IPN.[32] Although PVP's modest radical-scavenging qualities lessen the effect of hydroxyl radicals on the polymer, the network stability is improved by hydrogen bonding between the lactam carbonyl groups of PVP and the PVA-CA matrix.[32,64] Additionally, PVP is well-entangled and successfully retained within the cross-linked network, as evidenced by the minimal weight loss observed in the Soxhlet assays for PVA-CA:PVP0.25. This structural stability improves the membrane resistance to oxidative degradation by reducing excessive swelling and water absorption and prevents reactive species from deeply permeating the membrane.[32,64]

As PVP content increases beyond 0.25, oxidative stability declines, dropping to 70.97% for PVA-CA:PVP1.5. This decrease correlates with the increase in weight loss in the Soxhlet test, reflecting the leaching of excess PVP that is poorly integrated into the matrix. Excess PVP disrupts the crosslinking network, destabilizes the semi-IPN and significantly increases swelling and water absorption.[22,32,68] This leads to increased hydrophilicity and porosity, allowing oxidants to penetrate deeper into the membrane and accelerating its degradation. In addition, degradation of PVP, which is inherently less resistant to oxidative damage, contributes to the observed weight loss and decreased stability.[22,32,68] The increased swelling observed in these membranes further exacerbates membrane fragility by exposing a larger surface area to oxidizing agents, leading to increased structural damage, embrittlement and failure under harsh conditions.[22,32,68]

These findings confirm that PVA-CA:PVP0.25 is the most suitable composition for improving the durability and performance of ISMs in alkaline electrochemical applications, as it balances water absorption, swelling, and oxidation resistance while achieving optimal oxidative stability.

4.8 Ionic conductivity

The hydroxide conductivity of the produced ISMs, measured by EIS, demonstrates their ion transport capacity and correlates well with their structural properties, swelling behavior, and water uptake.[22,59] Since all membranes were alkali-treated with KOH, this process played an important role in improving hydroxide ion conductivity by modifying the polymer structure and increasing the availability of hydroxide ion transport pathways.[22,36] The alkali treatment improves the overall stability of the membrane by removing residual impurities, strengthening inter- and intramolecular hydrogen bonds, and increasing the density of hydroxyl groups. This chemical activation further improves ion solvation and transport, which are critical for ISMs in electrochemical applications.[22,36]

The limited water uptake (~60.09%) and lack of extra ionic channels in the neat PVA membrane result in a relatively low conductivity (~2.33 mS cm^{-1}) (Fig. 11a). Although limited ion transport is supported by the hydration layers around hydroxyl groups, conductivity is hindered by the absence of functional groups made especially for ion exchange.[22] Despite the stabilization and improved accessibility of the hydroxyl groups due to the alkaline treatment in KOH, neat PVA's hydroxide ion

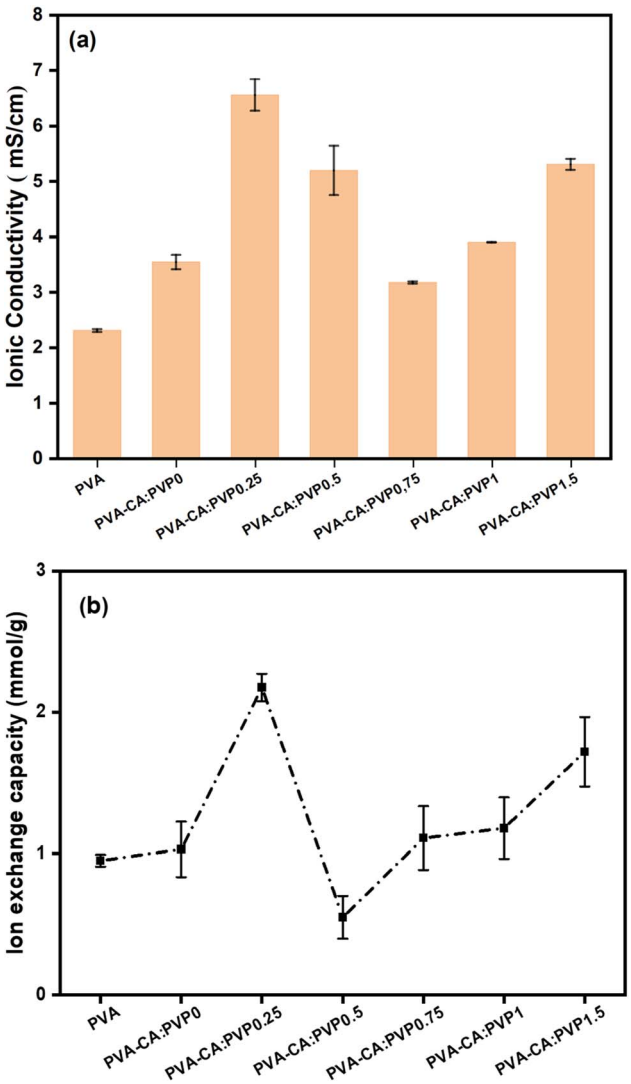

Fig. 11 (a) OH^- ionic conductivity and (b) ion exchange capacity of the prepared membranes.

conduction capabilities remain restricted in the absence of further structural alterations.[22] Upon crosslinking, the hydroxide conductivity increases to about 3.54 mS cm^{-1}. By creating a stable three-dimensional network and adding residual carboxylic groups (–COOH), the crosslinking process enhances ionic transport by creating more ionizable sites.[22] Crosslinks also improve the membrane's dimensional stability and mechanical strength, limiting excessive swelling while preserving enough water absorption for ion solvation. The polymer matrix is further strengthened by the ester linkages created during crosslinking, which also optimize ion transport conditions and restrict excessive hydration.[30–32]

The most significant improvement in conductivity (~6.56 mS cm^{-1}) was observed when PVP was added, the highest value among all membranes. This improvement was attributed to the formation of a stable semi-IPN between PVA-CA and PVP, where the lactam carbonyl groups (C=O) of PVP created additional ion channels and optimized water uptake (~193. 96%), which resulted in complete hydration of the ionic sites without excessive swelling.[32] Indeed, PVP increases the availability of hydrophilic functional groups, which makes it easier for the hydroxide ions to pass through the membrane and improves their solvation. The minimal weight loss given by Soxhlet extraction tests and high oxidative stability confirmed the structural stability of the semi-IPN membrane, indicating that it can effectively retain ionizable components.[32] The hydroxide conductivity drops dramatically to about 3.17 mS cm^{-1} as the PVP content rises to 0.75. The semi-IPN structure is broken, and the cross-linked matrix's ability to hold onto PVP is saturated, which causes this decrease.[32] Excess PVP reduces the homogeneity of ionic channels by forming poorly integrated microdomains. In addition, phase separation leads to a decrease in water uptake (~136.93%) in this region, as PVP-rich domains absorb water less efficiently, resulting in restricted hydroxide ion transport through decreased hydration.[32] At higher PVP content (ratios of 1 and 1.5), conductivity slightly increases to about 3.90 mS cm^{-1} and 5.35 mS cm^{-1}, respectively. The recovery of conductivity was associated with a re-increase in water uptake (~210.76%) due to the formation of highly hydrophilic PVP-rich microdomains.[22,32,68] These microdomains are partially compensate for the structural damage by improving water and ion transport pathways. However, the overall ion transport efficiency was limited due to the lack of a stable semi-IPN structure and the leaching of poorly incorporated PVP, as confirmed in Soxhlet and oxidative stability tests. Although conductivity was improved, the structural integrity of these membranes decreased, which may affect their long-term performance.[22,32,68]

The results indicate a notable enhancement in ionic conductivity through the introduction of citric acid and the optimization of PVP content. The optimized membrane (PVA-CA:PVP0.25) achieved a conductivity of 6.56 mS cm^{-1}, significantly higher than previously reported PVA-based membranes. In comparison, Lewandowski *et al.*[17] reported conductivity levels approaching 10^{-3} S cm^{-1}, while Palacios *et al.*[16] achieved a maximum conductivity of 2.3×10^{-3} S cm^{-1} for PVA-based alkaline membranes. This enhancement is attributed to the formation of a stable semi-IPN structure. Furthermore, the optimized water uptake (~193.96%) ensured efficient hydration of ionic sites without excessive swelling, highlighting the importance of material composition in maximizing ionic conductivity.

The results of IEC measurements confirm the trends observed in EIS, which quantifies the concentration of ion-exchangeable groups that directly affect hydroxide ion transport.[22,59] Due to the limited presence of functional hydroxyl groups, the pure PVA membrane exhibited a low IEC (~0.95 mmol g^{-1}) (Fig. 11b), which limited the ion exchange efficiency and resulted in low conductivity (~2.33 mS cm^{-1}). The introduction of citric acid slightly increased the IEC (~1.03 mmol g^{-1}) and improved the conductivity (~3.54 mS cm^{-1}) due to the additional ion exchange sites provided by the remaining carboxyl groups. However, the crosslinking network limited excessive swelling and maintained structural integrity.[65] The highest IEC value (~2.18 mmol g^{-1}) was achieved when PVP was added at a ratio of 0.25, corresponding to the highest conductivity (~6.56 mS cm^{-1}). As previously stated, the formation of a stable semi-IPN at this stage optimized hydration (~193.96%) and simultaneously prevented excessive swelling, enabling efficient ion exchange and hydroxide transport.[32] The presence of carbonyl groups in lactam PVP creates additional ion exchange sites, and the semi-IPN structure prevents the leaching of PVP as confirmed by the Soxhlet test.[65] Increasing PVP content to 0.5 resulted in a sharp decrease in IEC (~0.55 mmol g^{-1}), which is correlated with the observed decrease in conductivity (~3.17 mS cm^{-1}). Excess PVP disrupts the network and lowers the density of functional sites, while increasing PVP swelling and leaching.[32] At high PVP content (ratio of 1.5), IEC recovered slightly (~1.72 mmol g^{-1}) due to improved hydration, but excessive swelling and porosity affected the retention of ion-exchangeable groups.[32,65] The partial recovery of IEC coincided with an increase in conductivity (~5.35 mS cm^{-1}), indicating that while hydration is important, an optimal structural network is also essential for long-term performance maintenance.[32,65]

Overall, the IEC results support the EIS trends and demonstrate that the best balance between hydration, swelling control, and ion exchange sites is found at PVA-CA:PVP0.25, where the maximum conductivity is achieved. Hydroxide solvation is improved by the KOH treatment, nevertheless, excessive PVP causes structural instability, increased leaching, and decreased ion exchange efficiency in the absence of a stable polymeric structure. These results demonstrate that to reach high IEC, conductivity, and stability for efficient ISMs in electrochemical applications, PVP content and network crosslinking must be optimized.

To better illustrate the significance of these findings, Table 1 presents a direct comparison between the optimized semi-IPN membrane and the previously reported PVA-based membranes. The comparison reveals that the optimized membrane (PVA-CA:PVP0.25) exhibits superior IEC and competitive ionic conductivity compared to the conventional PVA/KOH membrane, thereby confirming the benefits of using a controlled semi-IPN system.

Table 1 Comparative properties of the prepared membrane and reported PVA-based membranes

Membrane	IEC (meq g^{-1})	Temperature (°C)	IC (mS cm^{-1})	Alkaline stability	References
PVA/KOH		20–25	1	Good stability, no degradation over 2 years in alkaline solution	17
PVA/KOH	0.95	20–25	47	Good electrochemical stability (±1.2 V)	69
PVA/Polyepichlorohydrin/KOH	0.86	20–25	20	Good chemical stability due to blending	70
PVA-poly(acrylonitrile-*co*-2-dimethylaminoethylmethacrylate)	1	20–25	3.43	Good stability in higher pH (pH > 7)	71
PVP-CA:PVP0.25	2.18	Room temperature	6.56	Good stability, no degradation after 3 months in 1 M KOH	This work

4.9 Thermal stability

The long-term success of ISMs in alkaline water electrolyzers depends on their ability to tolerate high temperatures without losing structural integrity or ion transport efficiency.[29] The effects of crosslinking, semi-IPNs formation, and post-treatment in KOH on the thermal resistance of these membranes are demonstrated by TGA and DTG analyses, which offer important insights into their degradation behavior. The membranes are subjected to high temperatures and a highly caustic environment during AWE, which could accelerate polymer deterioration if the network is not properly maintained.[29] By adding carboxylate ($-COO^-$) groups through the partial hydrolysis of ester bonds, the cooking process in KOH changes the membrane's ionic characteristics and affects its thermal stability. It also modulates polymer interaction and influences the decomposition behavior observed in TGA.[29,66,72]

Given the hydrophilic nature of the polymer matrix and its ability to retain moisture, all membranes show an initial weight loss between 50 °C and 150 °C, corresponding to the evaporation of absorbed water and volatile compounds.[73,74] TGA data (Fig. 12a) show that all membranes undergo a multi-stage degradation process, with Tonset (the initial decomposition temperature) and Tmax (the maximum decomposition temperature) acting as indicators of thermal stability.

The neat PVA membranes have high thermal stability with Tonset of 199.19 °C, Tmax1 (Fig. 12b) of 236.92 °C, and Tmax2 of 450.10 °C, indicating a densely packed polymer matrix supported by strong hydrogen bonding interactions. The first degradation phase (Tmax1) corresponds to the removal of bound water and degradation of the hydroxyl side groups, while the main degradation peak of Tmax2 represents the breakage of the polymer skeleton, which leads to CO_2 release.[73,74] The high Tonset and Tmax2 values reflect PVA's inherent thermal resistance, which is further enhanced by KOH doping. Alkali treatment leads to partial deacetylation and increased crystallinity, thus enhancing intermolecular interactions and preventing premature degradation.[29,66,72] These results are consistent with the high oxidative stability (98%) of PVA, as the dense hydrogen bonding network prevents free radical penetration and inhibits polymer degradation.

Crosslinking with citric acid (PVA-CA) results in a slight decrease in thermal stability, with Tonset falling to 197.64 °C, Tmax1 to 231.03 °C, and Tmax2 to 445.60 °C. This reduction is attributed to the introduction of thermally cleavable ester

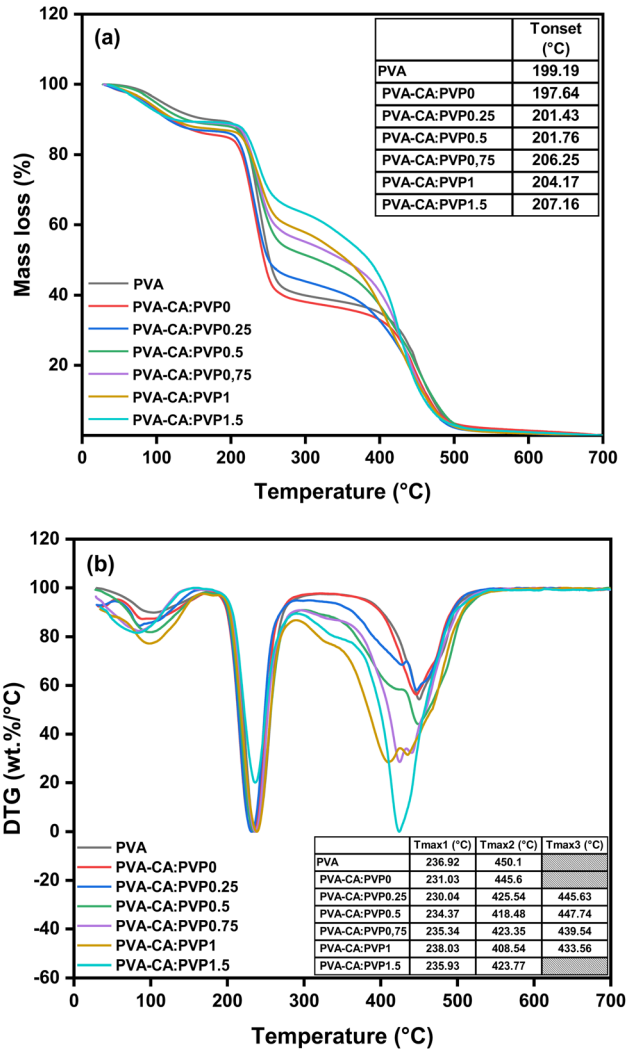

Fig. 12 Thermal stability of the produced ion-solvating membranes. (a) ATG curve, (b) DTG curve.

bonds in place of hydroxyl groups.[74,75] While cross-linking increases mechanical stiffness and limits swelling, it also introduces thermally unstable bonds, making the polymer network more susceptible to premature degradation.[74,75] The low Tmax2 further indicates that although esterification improves dimensional stability, the high-temperature stability of the polymer backbone is compromised.[74,75] Additionally, the absence of citric acid's characteristic endothermic peak (~156 °C), which corresponds to its melting point, confirms that citric acid was molecularly distributed through crosslinking with PVA.[76] This behavior aligns with the results of oxidative stability, which show that PVA-CA has poorer resistance (80%) than neat PVA since ester linkages are more vulnerable to oxidative and hydrolytic attack.

The inclusion of PVP in the membrane composition leads to a more complex degradation profile, reflecting the influence of the semi-IPN structure. A closer examination of the degradation steps shows that blending with PVP splits the second PVA degradation step into two distinct degradation stages.[73] This behavior implies that the addition of PVP modifies the interactions between the polymers, improves the thermal durability of the network through the formation of hydrogen bonds with PVA-CA, and delays the decomposition of the polymer backbone, thus modifying the thermal degradation pathway.[73,77] The observed change in thermal stability is also linked to the decrease in crystallinity due to the incorporation of PVP.[73] Since PVP is highly amorphous, its incorporation disrupts the ordered crystalline domains of PVA, thereby increasing the disorder of the polymer matrix. The addition of the amorphous phase improved chain mobility and initially stabilized the structure, but the introduction of excess PVP eventually weakened resistance to high temperatures.[73] As a result, all films of PVA-CA:PVPX blends showed three degradation phases instead of two, confirming the structural changes induced by the addition of PVP.

At low PVP content (PVA-CA:PVP0.25), Tonset increases to 201.43 °C, Tmax1 is 230.04 °C, Tmax2 is 425.54 °C, and the new Tmax3 appears at 445.63 °C. The slight increase in Tonset confirms that the introduction of PVP increases early-stage thermal stability, while Tmax3 indicates the progressive degradation of the semi-IPN structure, preventing rapid degradation of the material.[32,64] In addition, the increased amorphous phase in this composition improves flexibility and stress distribution, preserving membrane stability without compromising thermal resistance.[73] This composition also exhibits optimal oxidative stability (85%), as PVP improves resistance to oxidative radicals while maintaining a structurally robust network. The retention of PVP within the cross-linked structure, as confirmed by minimal weight loss in Soxhlet extraction tests, further supports these thermal improvements.

Thermal stability trends weaken above a PVP content of 0.25 wt%, with Tonset fluctuating and Tmax2 progressively declining. This suggests that excess PVP disrupts rather than strengthens the semi-IPN structure. In fact, the polymer matrix becomes more amorphous at higher PVP concentrations, resulting in weaker interactions between polymers and a decrease in intermolecular cohesion, thus accelerating polymer degradation.[73] For PVA-CA:PVP0.5, Tonset is 201.76 °C, Tmax1 increases to 234.37 °C, Tmax2 decreases to 418.48 °C and Tmax3 appears at 447.74 °C. Increasing PVP content leads to polymer phase separation, reducing high-temperature stability and network homogeneity, even though PVP initially increases early-stage thermal resistance.[31,34,35] A comparable pattern can be observed in PVA-CA:PVP0.75, where Tonset increases to 206.25 °C, Tmax1 reaches 235.34 °C, while Tmax2 falls even lower to 423.35 °C, and Tmax3 rises to 439.54 °C. These results are consistent with oxidative stability trends, which show that increasing membrane porosity due to excessive PVP inclusion leads to a decrease in oxidative durability.

At even higher PVP concentrations (PVA-CA:PVP1 and PVA-CA:PVP1.5), thermal stability further declines, confirming that excessive PVP weakens polymer cohesion. For PVA-CA:PVP1, Tonset decreases slightly to 204.17 °C, Tmax1 reaches its highest value at 238.03 °C, but Tmax2 significantly drops to 408.54 °C, with Tmax3 at 433.56 °C. According to this peak shift, PVP increases initial thermal resistance, but as it contains weakly bonded PVP chains, it accelerates backbone disintegration at higher temperatures.[73] Similar to this, PVA-CA:PVP1.5 shows a somewhat higher Tonset of 207.16 °C, with Tmax1 at 235.93 °C and Tmax2 at 423.77 °C. However, the phase instability still exists because excessive PVP compromises the semi-IPN's structural integrity. The decrease in Tmax2 implies that weaker polymer domains produced by unbound PVP are more likely to degrade prematurely.[22,32,68] This behavior is consistent with oxidative stability results, where PVP concentrations above 0.25 lead to reduced oxidative resistance (60%), increased polymer leaching (Soxhlet extraction), and increased vulnerability to oxidative and thermal degradation.

Overall, the effects of polymer composition, cross-linking, semi-IPN formation, and KOH post-treatment on thermal stability are demonstrated by TGA and DTG data. By reducing crystallinity, the incorporation of PVP initially improves flexibility and stress distribution; however, excessive amounts of amorphous material reduce thermal resistance. Due to its stable semi-IPN structure, PVA-CA:PVP0.25 achieves the optimum balance between thermal and oxidative stability. Although KOH treatment improves ionic functions, phase separation weakens polymer cohesion and accelerates degradation at high PVP concentrations. These results demonstrate that, while high PVP concentrations are detrimental to long-term stability in electrochemical media, moderate PVP concentrations improve thermal performance.

4.10 Tensile analysis

The overall performance of ISMs, their processability and durability in AWE are all strongly influenced by their mechanical characteristics. Stiffness, tensile strength and ductility must be balanced to avoid mechanical deterioration, creep or rupture during use.[65,66] Whereas too much flexibility can lead to dimensional instability and swelling, ultimately reducing conductivity and performance, too much stiffness can induce brittleness and fracture.[65,66] These characteristics are strongly influenced by the creation of semi-IPN and by post-processing

procedures, notably thermal curing and KOH doping, which reinforce polymer cohesion, maximize cross-linking density and control swelling.

The evolution of Young's modulus across the membrane compositions shows how cross-linking, semi-IPN creation, KOH treatment and the switch from a PVA-rich to a PVP-rich structure affect membrane stiffness (Fig. 13). Neat PVA exhibits moderate stiffness (807.96 MPa), which is mainly due to the strong hydrogen bonds between the hydroxyl groups that allow a certain degree of chain mobility mainly due to the post-treatment, as previously explained.[65,66] Young's modulus increases by 105% when citric acid (PVA-CA:PVP0) is used for crosslinking, as ester bonds strengthen the network by limiting molecular mobility.[56,78] In fact, by encouraging more cross-linking interactions and inducing partial deacetylation, thermal curing and alkaline treatment strengthen interactions between polymers, thereby increasing rigidity.[56,78] This is in agreement with SEM images, which reveal a more compact and dense structure after crosslinking. However, Young's modulus slightly decreases by 23% when PVP is added at 0.25 wt% (PVA-CA:PVP0.25), while SEM images reveal a modest increase in porosity and surface roughness, indicating the plasticizing impact of PVP. By physically trapping PVP within the PVA-CA network and balancing rigidity and flexibility, PVP's hydrophilic lactam groups break the dense hydrogen-bonded structure of PVA, ensuring the creation of a stable semi-IPN.[30–32] When the PVP content exceeds this threshold, the membranes transition from a PVA-rich to a PVP-rich system, resulting in phase separation and weaker network interactions, thus initially reducing Young's modulus (PVA-CA:PVP0.5: 1038.12 MPa).[34,35] Nevertheless, Young's modulus increases again (to 1425 MPa) with higher PVP contents (PVA-CA:PVP0.75 to PVA-CA:PVP1.5), indicating that excess PVP begins to create its own interpolymer network, adding rigidity while decreasing overall homogeneity.[34,35] This is consistent with SEM data, which show that at higher concentrations of PVP, morphology reverts to a denser, more uniform appearance.

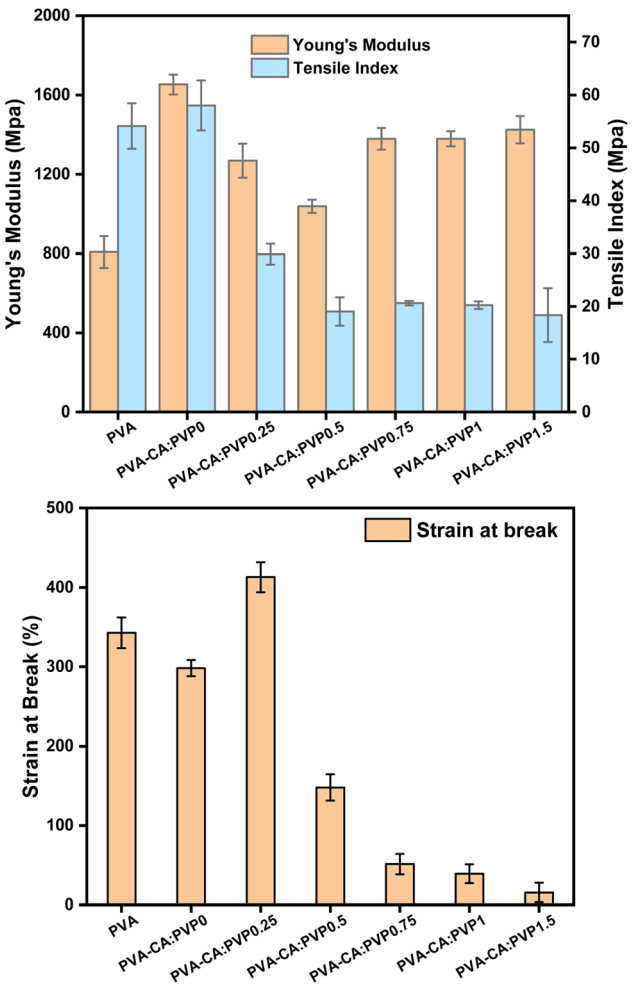

Fig. 13 Mechanical properties of the prepared ion-solvating membranes.

The tensile strength of membranes provides information on interchain interactions and polymer adhesion, as well as the ability of the network to tolerate stress before failure. Due to strong hydrogen bonding between hydroxyl groups and tight molecular packing, neat PVA has a high tensile strength of 54.14 MPa.[65,66] The latter increases by around 7% after cross-linking with citric acid (PVA-CA:PVP0), as the rigid cross-linked structure improves load-bearing capacity by limiting polymer chain mobility.[56,78] Furthermore, during partial ester hydrolysis, KOH doping adds carboxylate groups ($-COO^-$), which alters the polymer matrix by reducing the polymer–polymer interactions, leading to mechanical weakness in subsequent compositions.[56,78] The introduction of PVP at 0.25 wt% (PVA-CA:PVP0.25) results in a tensile strength drop to 29.88 MPa, as semi-IPN formation disrupts chain packing, reducing the force required for failure.[34,35] This effect becomes more pronounced as PVP content increases, leading to a further decline in tensile strength (PVA-CA:PVP0.5: 19.04 MPa, PVA-CA:PVP1.5: 18.36 MPa). In fact, excess PVP weakens interpolymer cohesion and disrupts matrix homogeneity by causing phase separation. When transitioning from PVA-rich to a PVP-rich membrane, weakly bonded PVP domains with low interchain reinforcement are formed, increasing polymer heterogeneity and decreasing tensile strength.[79]

The findings of the strain at break demonstrate the membranes' elongation and flexibility capacity. Neat PVA has a relatively high strain at break (342.73%), demonstrating its inherent flexibility, which results from strong but dynamic hydrogen bonding, thus enabling polymer chains to stretch widely before breaking.[65,66] Citric acid crosslinking (PVA-CA:PVP0) reduces strain at break to 298.23% because the creation of a stiff three-dimensional network limits the mobility of the polymer. KOH doping further stabilizes the network by reinforcing the structure through partial deacetylation and additional crosslinking, but at the same time, it slightly limits chain elongation due to the increased rigidity of the polymer matrix.[56,78] At PVA-CA:PVP0.25, strain at break increases significantly to 412.81%, marking the formation of a semi-IPN, where PVP's plasticizing effect enhances flexibility by disrupting interpolymer interactions, allowing greater elongation before rupture.[73] However, ductility drastically decreases beyond

0.25 wt% PVP (PVA-CA:PVP0.5: 147.97%, PVA-CA:PVP1.5: 15.44%), indicating that excess PVP compromises network cohesion, decreased flexibility, and increased brittleness. The transition from a PVA-rich to a PVP-rich structure results in phase-separated microdomains, which weaken the matrix and disrupt the uniform distribution of stress, accelerating failure under tensile load.[34,35] These results show that although PVP improves ductility at low concentrations, over-incorporation compromises network integrity and increases the membranes' susceptibility to mechanical failure under tensile stress.

Overall, these mechanical trends align with SEM observations, confirming that a moderate PVP concentration (PVA-CA:PVP0.25) optimally balances mechanical strength and flexibility, making it the most mechanically robust and durable composition for ion-exchange membranes in AWE.

5 Conclusion

This study successfully developed a novel semi-IPN membrane for AWE by combining PVA cross-linked with citric acid and physically entangled with PVP. The manufacturing process included solvent casting, thermal curing at 130 °C to strengthen the crosslinking, and KOH doping to improve the hydroxide ion conductivity and the overall membrane performance. The semi-IPN structure effectively preserved the integrity of the polymer matrix while optimizing entanglement to enhance mechanical strength, water retention, and ion transport. The results highlighted that careful tuning of PVP concentration was crucial to achieve a balance between polymer entanglement and structural stability, avoiding issues such as excessive phase separation and increased swelling, while also ensuring good ionic conductivity for high performance in AWE.

Among the various formulations tested, the PVA-CA:PVP0.25 membrane exhibited the best combination of structural integrity, ionic conductivity, and chemical stability. Thermal curing at 130 °C enhanced the polymer network, improving the durability of the membrane with a rigidity of 1270 MPa and a ductility of 413%. This membrane achieved a water uptake of 193.96%, ensuring a balance between preventing excessive swelling and maintaining adequate hydration for effective ion conduction. KOH doping enhanced the ionic conductivity (6.56 mS cm^{-1} at room temperature) by introducing carboxylate functional groups ($-COO^-$), which further improved the mobility of hydroxide ions. The membrane demonstrated long-term stability by maintaining structural durability for more than three months under alkaline conditions, while oxidative stability tests showed a 90.9% mass retention after eight hours. Additionally, its enhanced thermal stability ensures reliable performance under elevated electrochemical operating temperatures.

Overall, these findings demonstrate the effectiveness of the semi-IPN approach in developing durable, high-performance ISM for alkaline environments. The optimized membrane combines superior mechanical properties and ion conduction with a scalable fabrication process, supporting its potential use in AWE. The results pave the way for future advancements in membrane design by emphasizing the importance of post-processing methods, doping strategies, and polymer network architecture in enhancing the stability and performance of ISMs for large-scale hydrogen production. This study focuses on membrane-level characterization under alkaline conditions, and future work will integrate these membranes into full-cell alkaline electrolyzer systems to evaluate performance and durability under practical operating conditions.

Conflicts of interest

The authors declare that they have no known competing financial interests or personal relationships that could have appeared to influence the work reported in this paper.

Data availability

The data that support the findings of this study are available from the corresponding author, Fatima-Zahra SEMLALI, upon reasonable request.

Acknowledgements

This study is supported by the Office Cherifien des Phosphates (OCP S.A.) in the Moroccan Kingdom along with funding provided by the UM6P-MSN University through the Bi-national energy initiative.

References

1 J. Jang, Y. Kang, J. H. Han, K. Jang, C. M. Kim and I. S. Kim, Developments and future prospects of reverse electrodialysis for salinity gradient power generation: Influence of ion exchange membranes and electrodes, *Desalination*, 2020, **491**, 114540, DOI: 10.1016/j.desal.2020.114540.

2 D. G. Caglayan, N. Weber, H. U. Heinrichs, J. Linßen, M. Robinius, P. A. Kukla and D. Stolten, Technical potential of salt caverns for hydrogen storage in Europe, *Int. J. Hydrogen Energy*, 2020, **45**, 6793–6805, DOI: 10.1016/j.ijhydene.2019.12.161.

3 M. Liu, X. Hu, B. Hu, L. Liu and N. Li, Soluble poly(aryl piperidinium) with extended aromatic segments as anion exchange membranes for alkaline fuel cells and water electrolysis, *J. Memb. Sci.*, 2022, **642**, 119966, DOI: 10.1016/j.memsci.2021.119966.

4 R. Abbasi, B. P. Setzler, S. Lin, J. Wang, Y. Zhao, H. Xu, B. Pivovar, B. Tian, X. Chen, G. Wu and Y. Yan, A Roadmap to Low-Cost Hydrogen with Hydroxide Exchange Membrane Electrolyzers, *Adv. Mater.*, 2019, **31**, 1–14, DOI: 10.1002/adma.201805876.

5 A. Buttler and H. Spliethoff, Current status of water electrolysis for energy storage, grid balancing and sector coupling via power-to-gas and power-to-liquids: A review, *Renew. Sustain. Energy Rev.*, 2018, **82**, 2440–2454, DOI: 10.1016/j.rser.2017.09.003.

6 B. Hu, Y. Huang, L. Liu, X. Hu, K. Geng, Q. Ju, M. Liu, J. Bi, S. Luo and N. Li, A stable ion-solvating PBI electrolyte enabled by sterically bulky naphthalene for alkaline water

electrolysis, *J. Memb. Sci.*, 2022, **643**, 120042, DOI: 10.1016/j.memsci.2021.120042.

7 X. Hu, Y. Huang, L. Liu, Q. Ju, X. Zhou, X. Qiao, Z. Zheng and N. Li, Piperidinium functionalized aryl ether-free polyaromatics as anion exchange membrane for water electrolysers: Performance and durability, *J. Memb. Sci.*, 2021, **621**, 118964, DOI: 10.1016/j.memsci.2020.118964.

8 Y. Du, L. Gao, L. Hu, M. Di, X. Yan, B. An and G. He, The synergistic effect of protonated imidazole-hydroxyl-quaternary ammonium on improving performances of anion exchange membrane assembled flow batteries, *J. Memb. Sci.*, 2020, **603**, 118011, DOI: 10.1016/j.memsci.2020.118011.

9 D. Li, A. R. Motz, C. Bae, C. Fujimoto, G. Yang, F. Y. Zhang, K. E. Ayers and Y. S. Kim, Durability of anion exchange membrane water electrolyzers, *Energy Environ. Sci.*, 2021, **14**, 3393–3419, DOI: 10.1039/d0ee04086j.

10 A. Khataee, A. Shirole, P. Jannasch, A. Krüger and A. Cornell, Anion exchange membrane water electrolysis using Aemion™ membranes and nickel electrodes, *J. Mater. Chem. A*, 2022, **10**, 16061–16070, DOI: 10.1039/d2ta03291k.

11 W. You, K. J. T. Noonan and G. W. Coates, Alkaline-stable anion exchange membranes: A review of synthetic approaches, *Prog. Polym. Sci.*, 2020, **100**, 101177, DOI: 10.1016/j.progpolymsci.2019.101177.

12 A. Dayan, M. L. A. Trisno, C. Yang, M. R. Kraglund, M. R. Almind, J. Hjelm, J. O. Jensen, D. Aili, H. S. Park and D. Henkensmeier, Quaternary Ammonium-Free Membranes for Water Electrolysis with 1 m KOH, *Adv. Energy Mater.*, 2023, **13**, 1–10, DOI: 10.1002/aenm.202302966.

13 M. R. Kraglund, M. Carmo, G. Schiller, S. A. Ansar, D. Aili, E. Christensen and J. O. Jensen, Ion-solvating membranes as a new approach towards high rate alkaline electrolyzers, *Energy Environ. Sci.*, 2019, **12**, 3313–3318, DOI: 10.1039/c9ee00832b.

14 B. Xing, and O. Savadogo, *Hydrogen R Oxygen Polymer Electrolyte Membrane Fuel Cells Ž PEMFCs/Based on Alkaline-Doped Polybenzimidazole Ž PBI/*, 2000, 697–702.

15 S. Guinot, E. Salmon, J. F. Penneau and J. F. Fauvarque, A new class of PEO-based SPEs: Structure, conductivity and application to alkaline secondary batteries, *Electrochim. Acta*, 1998, **43**, 1163–1170, DOI: 10.1016/S0013-4686(97)10015-9.

16 I. Palacios, R. Castillo and R. A. Vargas, Thermal and transport properties of the polymer electrolyte based on poly(vinyl alcohol)-KOH-H2O, *Electrochim. Acta*, 2003, **48**, 2195–2199, DOI: 10.1016/S0013-4686(03)00204-4.

17 A. Lewandowski, K. Skorupska and J. Malinska, Novel poly(vinyl alcohol)-KOH-H2O alkaline polymer electrolyte, *Solid State Ionics*, 2000, **133**, 265–271, DOI: 10.1016/S0167-2738(00)00733-5.

18 L. A. Diaz, R. E. Coppola, G. C. Abuin, R. Escudero-Cid, D. Herranz and P. Ocón, Alkali-doped polyvinyl alcohol – Polybenzimidazole membranes for alkaline water electrolysis, *J. Memb. Sci.*, 2017, **535**, 45–55, DOI: 10.1016/j.memsci.2017.04.021.

19 S. Alipoori, S. Mazinani, S. H. Aboutalebi and F. Sharif, Review of PVA-based gel polymer electrolytes in flexible solid-state supercapacitors: Opportunities and challenges, *J. Energy Storage*, 2020, **27**, 101072, DOI: 10.1016/j.est.2019.101072.

20 L. Lebrun, N. Follain and M. Metayer, Elaboration of a new anion-exchange membrane with semi-interpenetrating polymer networks and characterisation, *Electrochim. Acta*, 2004, **50**, 985–993, DOI: 10.1016/j.electacta.2004.07.040.

21 S. Amnuaypanich, J. Patthana and P. Phinyocheep, Mixed matrix membranes prepared from natural rubber/poly(vinyl alcohol) semi-interpenetrating polymer network (NR/PVA semi-IPN) incorporating with zeolite 4A for the pervaporation dehydration of water-ethanol mixtures, *Chem. Eng. Sci.*, 2009, **64**, 4908–4918, DOI: 10.1016/j.ces.2009.07.028.

22 J. Qiao, J. Fu, R. Lin, J. Ma and J. Liu, Alkaline solid polymer electrolyte membranes based on structurally modi fi ed PVA/PVP with improved alkali stability, *Polymer (Guildf.)*, 2010, **51**, 4850–4859, DOI: 10.1016/j.polymer.2010.08.018.

23 C. Danielli, L. van Langen, D. Boes, F. Asaro, S. Anselmi, F. Provenza, M. Renzi and L. Gardossi, 2,5-Furandicarboxaldehyde as a bio-based crosslinking agent replacing glutaraldehyde for covalent enzyme immobilization, *RSC Adv.*, 2022, **12**, 35676–35684, DOI: 10.1039/d2ra07153c.

24 J. Y. Lim, D. A. Kang, N. U. Kim, J. M. Lee and J. H. Kim, Bicontinuously crosslinked polymer electrolyte membranes with high ion conductivity and mechanical strength, *J. Memb. Sci.*, 2019, **589**, 117250, DOI: 10.1016/j.memsci.2019.117250.

25 X. Chen, Y. Zhan, J. Tang, X. Yang, A. Sun, B. Lin, F. Zhu, H. Jia and X. Lei, Advances in high performance anion exchange membranes: Molecular design, preparation methods, and ion transport dynamics, *J. Environ. Chem. Eng.*, 2023, **11**, 110749, DOI: 10.1016/j.jece.2023.110749.

26 C. Hirschl, L. Neumaier, S. Puchberger, W. Mühleisen, G. Oreski, G. C. Eder, R. Frank, M. Tranitz, M. Schoppa, M. Wendt, N. Bogdanski, A. Plösch and M. Kraft, Determination of the degree of ethylene vinyl acetate crosslinking via Soxhlet extraction: Gold standard or pitfall?, *Sol. Energy Mater. Sol. Cells*, 2015, **143**, 494–502, DOI: 10.1016/j.solmat.2015.07.043.

27 T. Y. Guo, Q. H. Zeng, C. H. Zhao, Q. L. Liu, A. M. Zhu and I. Broadwell, Quaternized polyepichlorohydrin/PTFE composite anion exchange membranes for direct methanol alkaline fuel cells, *J. Memb. Sci.*, 2011, **371**, 268–275, DOI: 10.1016/j.memsci.2011.01.043.

28 D. S. Haryadi, Development of composite membranes of PVA-TEOS doped KOH for alkaline membrane fuel cell, *AIP Conf. Proc.*, 2015, **1699**, 040016, DOI: 10.1063/1.4938331.

29 A. M. Samsudin and M. Bodner, A Brief Review of Poly (Vinyl Alcohol) -Based Anion Exchange Membranes for Alkaline, *Fuel Cells*, 2022, 1–26.

30 A. Zakrzewska, S. S. Zargarian, C. Rinoldi, A. Gradys, D. Jarząbek, M. Zanoni, C. Gualandi, M. Lanzi and F. Pierini, Electrospun Poly(vinyl alcohol)-Based

Conductive Semi-interpenetrating Polymer Network Fibrous Hydrogel: A Toolbox for Optimal Cross-Linking, *ACS Mater. Au*, 2023, **3**, 464–482, DOI: 10.1021/acsmaterialsau.3c00025.

31 Q. B. Wei, Y. L. Luo, L. J. Gao, Q. Wang and D. J. Wang, Synthesis, characterization and swelling kinetics of thermoresponsive PAM-g-PVA/PVP semi-IPN hydrogels, *Polym. Sci. – Ser. A*, 2011, **53**, 707–714, DOI: 10.1134/S0965545X11080062.

32 Y. Ye, J. Rick and B. Hwang, Water Soluble Polymers as Proton Exchange Membranes for Fuel a Cells, *Polymers*, 2012, 913–963, DOI: 10.3390/polym4020913.

33 A. Himawan, Q. K. Anjani, U. Detamornrat, L. K. Vora, A. D. Permana, R. Ghanma, Y. Naser, D. Rahmawanty, C. J. Scott and R. F. Donnelly, Multifunctional low temperature-cured PVA/PVP/citric acid-based hydrogel forming microarray patches: Physicochemical characteristics and hydrophilic drug interaction, *Eur. Polym. J.*, 2023, **186**, 111836, DOI: 10.1016/j.eurpolymj.2023.111836.

34 F. L. Rashid and A. Hashim, Structural , Swelling and Water Absorption Properties of New Polymer Blends for Modern Applications Structural , Swelling and Water Absorption Properties of New Polymer Blends for Modern Applications, Nanosistemi, *Nanomater. Nanotehnologii*, 2022, **19**, 905–912.

35 S. E. Kudaibergenov, N. Dolya, G. Tatykhanova, Z. E. Ibraeva and B. K. Musabaeva, Semi-interpenetrating Polymer Networks of Polyelectrolytes, *Eurasian Chem.-Technol. J.*, 2007, **9**, 177–192.

36 M. Makrygianni, S. Aivali, Y. Xia, M. R. Kraglund, D. Aili and V. Deimede, Polyisatin derived ion-solvating blend membranes for alkaline water electrolysis, *J. Memb. Sci.*, 2023, **669**, 121331, DOI: 10.1016/j.memsci.2022.121331.

37 D. R. Baganizi, E. Nyairo, S. A. Duncan, S. R. Singh and V. A. Dennis, Interleukin-10 conjugation to carboxylated PVP-coated silver nanoparticles for improved stability and therapeutic efficacy, *Nanomaterials*, 2017, **7**, 165, DOI: 10.3390/nano7070165.

38 E. M. Abdelrazek, G. El Damrawi and A. Al-Shahawy, Some studies on calcium phosphate embedded in polyvinyl alcohol matrix before and after γ-irradiation, *Phys. B Condens. Matter*, 2010, **405**, 808–816, DOI: 10.1016/j.physb.2009.06.129.

39 S. R. Sudhamani, M. S. Prasad and K. Udaya Sankar, DSC and FTIR studies on Gellan and polyvinyl alcohol (PVA) blend films, *Food Hydrocoll*, 2003, **17**, 245–250, DOI: 10.1016/S0268-005X(02)00057-7.

40 I. M. Jipa, A. Stoica, M. Stroescu, L. M. Dobre, T. Dobre, S. Jinga and C. Tardei, Potassium sorbate release from poly(vinyl alcohol)-bacterial cellulose films, *Chem. Pap.*, 2012, **66**, 138–143, DOI: 10.2478/s11696-011-0068-4.

41 S. Mallakpour and N. Jarang, Production of bionanocomposites based on poly(vinyl pyrrolidone) using modified TiO2 nanoparticles with citric acid and ascorbic acid and study of their physicochemical properties, *Polym. Bull.*, 2018, **75**, 1441–1456, DOI: 10.1007/s00289-017-2100-5.

42 A. Mukharya, N. Mansuri, S. Chaudhary and A. Misra, Solid-state characterization of lacidipine/PVP K 29/32 solid dispersion primed by solvent co-evaporation, *Int. J. Pharm. Investig.*, 2012, **2**, 90, DOI: 10.4103/2230-973x.100048.

43 K. El Bourakadi, F. Z. Semlali, M. Hammi and M. El Achaby, A review on natural cellulose fiber applications: Empowering industry with sustainable solutions, *Int. J. Biol. Macromol.*, 2024, **281**, 135773, DOI: 10.1016/j.ijbiomac.2024.135773.

44 A. Bahloul, F. Z. Semlali, M. Oumam, H. Hannache, Z. Kassab and M. El Achaby, Starch bio-nanocomposites based on phosphorylated and sulphated cellulose nanocrystals extracted from pepper plant residue: effect of surface functionality on property improvements, *Cellulose*, 2023, 5051–5070, DOI: 10.1007/s10570-023-05199-4.

45 M. H. Salim, Z. Kassab, E. Ablouh, F. Semlali Aouragh Hassani and M. El Achaby, Cellulosic biocomposite foam papers impregnated by crosslinked starch/poly (vinyl alcohol) biopolymers, *Ind. Crop. Prod.*, 2023, **192**, 116074, DOI: 10.1016/j.indcrop.2022.116074.

46 F. Yan, K. Mukherjee, M. Maroncelli and H. J. Kim, Infrared Spectroscopy of Li+ Solvation in Diglyme: Ab Initio Molecular Dynamics and Experiment, *J. Phys. Chem. B*, 2023, **127**, 9191–9203, DOI: 10.1021/acs.jpcb.3c05612.

47 Z. Niavarani, D. Breite, A. Prager, I. Thomas, M. Kuehnert, B. Abel, R. Gläser and A. Schulze, Synthesis of composite imprinted polymer membranes for the selective removal of 17β-estradiol from water, *Mater. Chem. Front.*, 2023, **7**, 4460–4472, DOI: 10.1039/d3qm00345k.

48 H. Abral, A. Atmajaya, M. Mahardika, F. Hafizulhaq, Kadriadi, D. Handayani, S. M. Sapuan and R. A. Ilyas, Effect of ultrasonication duration of polyvinyl alcohol (PVA) gel on characterizations of PVA film, *J. Mater. Res. Technol.*, 2020, **9**, 2477–2486, DOI: 10.1016/j.jmrt.2019.12.078.

49 M. M. Ghobashy, D. M. Alshangiti, S. A. Alkhursani, S. A. Al-Gahtany, F. S. Shokr and M. Madani, Improvement of in Vitro Dissolution of the Poor Water-Soluble Amlodipine Drug by Solid Dispersion with Irradiated Polyvinylpyrrolidone, *ACS Omega*, 2020, **5**, 21476–21487, DOI: 10.1021/acsomega.0c01910.

50 D. Nataraj, R. Reddy and N. Reddy, Crosslinking electrospun poly (vinyl) alcohol fibers with citric acid to impart aqueous stability for medical applications, *Eur. Polym. J.*, 2020, **124**, 109484, DOI: 10.1016/j.eurpolymj.2020.109484.

51 R. Liu and W. Li, High-Thermal-Stability and High-Thermal-Conductivity Ti3C2T x MXene/Poly(vinyl alcohol) (PVA) Composites, *ACS Omega*, 2018, **3**, 2609–2617, DOI: 10.1021/acsomega.7b02001.

52 E. Rynkowska, K. Fatyeyeva, and J. Kujawa, *Chemically and Thermally Crosslinked PVA-Based Membranes : Effect on Swelling and*, 2019, 7–9.

53 L. L. Xia, C. L. Li and Y. Wang, In-situ crosslinked PVA/organosilica hybrid membranes for pervaporation separations, *J. Memb. Sci.*, 2016, **498**, 263–275, DOI: 10.1016/j.memsci.2015.10.025.

54 C. C. Tsai, R. J. Wu, H. Y. Cheng, S. C. Li, Y. Y. Siao, D. C. Kong and G. W. Jang, Crystallinity and dimensional stability of biaxial oriented poly(lactic acid) films, *Polym. Degrad. Stab.*, 2010, **95**, 1292–1298, DOI: 10.1016/j.polymdegradstab.2010.02.032.

55 J. Wu, R. P. Chandra, K. H. Kim, C. S. Kim, Y. Pu, A. J. Ragauskas and J. N. Saddler, Enhancing Enzyme-Mediated Hydrolysis of Mechanical Pulps by Deacetylation and Delignification, *ACS Sustain. Chem. Eng.*, 2020, **8**, 5847–5855, DOI: **10.1021/acssuschemeng.9b07226**.

56 S. M. Huang, S. M. Liu, H. Y. Tseng and W. C. Chen, Effect of Citric Acid on Swelling Resistance and Physicochemical Properties of Post-Crosslinked Electrospun Polyvinyl Alcohol Fibrous Membrane, *Polymers*, 2023, **15**, 1738, DOI: **10.3390/polym15071738**.

57 Y. B. Truong, J. Choi, J. Mardel, Y. Gao, S. Maisch, M. Musameh and I. L. Kyratzis, Functional Cross-Linked Electrospun Polyvinyl Alcohol Membranes and Their Potential Applications, *Macromol. Mater. Eng.*, 2017, **302**, 1–9, DOI: **10.1002/mame.201700024**.

58 J. Qian, C. Wang, X. Zhang, J. Hu, X. Zhao, J. Li and Q. Ren, Synthesis and properties of anion exchange membranes with dense multi-cations and flexible side chains for water electrolysis, *J. Power Sources*, 2023, **564**, 232877, DOI: **10.1016/j.jpowsour.2023.232877**.

59 L. Liu, H. Ma, M. Khan and B. S. Hsiao, Recent Advances and Challenges in Anion Exchange Membranes Development/Application for Water Electrolysis: A Review, *Membranes*, 2024, **14**, 85, DOI: **10.3390/membranes14040085**.

60 J. Ran, L. Wu, Y. He, Z. Yang, Y. Wang, C. Jiang, L. Ge, E. Bakangura and T. Xu, Ion exchange membranes: New developments and applications, *J. Memb. Sci.*, 2017, **522**, 267–291, DOI: **10.1016/j.memsci.2016.09.033**.

61 X. Hu, M. Liu, Y. Huang, L. Liu and N. Li, Sulfonate-functionalized polybenzimidazole as ion-solvating membrane toward high-performance alkaline water electrolysis, *J. Memb. Sci.*, 2022, **663**, 121005, DOI: **10.1016/j.memsci.2022.121005**.

62 A. Hasimi, A. Stavropoulou, K. G. Papadokostaki and M. Sanopoulou, Transport of water in polyvinyl alcohol films: Effect of thermal treatment and chemical crosslinking, *Eur. Polym. J.*, 2008, **44**, 4098–4107, DOI: **10.1016/j.eurpolymj.2008.09.011**.

63 J. Wu, Z. Wang, W. Yan, Y. Wang, J. Wang and S. Wang, Improving the hydrophilicity and fouling resistance of RO membranes by surface immobilization of PVP based on a metal-polyphenol precursor layer, *J. Memb. Sci.*, 2015, **496**, 58–69, DOI: **10.1016/j.memsci.2015.08.044**.

64 C. M. R. Madhuranthakam, W. S. K. Abudaqqa, and M. Fowler, Advances in Polyvinyl Alcohol-Based Membranes for Fuel Cells : A Comprehensive Review on Types, *Synthesis , Modifications , and Performance Optimization*, 2024.

65 A. F. Elerian, A. A. Mohamed, E. M. Elnaggar and M. A. A. Saied, Development of novel proton exchange membranes based on cross - linked polyvinyl alcohol (PVA)/5 - sulfosalicylic acid (SSCA) for fuel cell applications, *Discov. Appl. Sci.*, 2024, 65–341, DOI: **10.1007/s42452-024-05940-z**.

66 G. Merle, M. Wessling and K. Nijmeijer, Anion exchange membranes for alkaline fuel cells : A review, *J. Membr. Sci.*, 2011, **377**, 1–35, DOI: **10.1016/j.memsci.2011.04.043**.

67 P. Kulasekaran, B. M. Mahimai and P. Deivanayagam, Novel cross-linked poly(vinyl alcohol)-based electrolyte membranes for fuel cell applications, *RSC Adv.*, 2020, 26521–26527, DOI: **10.1039/d0ra04360e**.

68 R. M. Santos, G. Mertens, M. Salman, Ö. Cizer and T. Van Gerven, Comparative study of ageing, heat treatment and accelerated carbonation for stabilization of municipal solid waste incineration bottom ash in view of reducing regulated heavy metal/metalloid leaching, *J. Environ. Manage.*, 2013, **128**, 807–821, DOI: **10.1016/j.jenvman.2013.06.033**.

69 C. C. Yang and S. J. Lin, Preparation of composite alkaline polymer electrolyte, *Mater. Lett.*, 2002, **57**, 873–881, DOI: **10.1016/S0167-577X(02)00888-1**.

70 C. C. Yang, S. J. Lin and S. T. Hsu, Synthesis and characterization of alkaline polyvinyl alcohol and poly(epichlorohydrin) blend polymer electrolytes and performance in electrochemical cells, *J. Power Sources*, 2003, **122**, 210–218, DOI: **10.1016/S0378-7753(03)00429-4**.

71 M. Kumar, S. Singh, and V. K. Shahi, *Based Anion-Exchange Membranes in Aqueous Media*, 2010, 198–206.

72 C. Tsioptsias, D. Fardis, X. Ntampou, I. Tsivintzelis and C. Panayiotou, Thermal Behavior of Poly(vinyl alcohol) in the Form of Physically Crosslinked Film, *Polymers*, 2023, **15**, 1843, DOI: **10.3390/polym15081843**.

73 N. Azeez Betti, Thermogravimetric Analysis on PVA/PVP Blend Under Air Atmosphere, *Eng. Technol. J.*, 2016, **34**, 2433–2442, DOI: **10.30684/etj.34.13a.6**.

74 L. C. Pittol, V. Z. Kieffer, E. L. Francisquetti and R. M. C. Santana, Evaluation of the effect of citric acid on the crosslinking of PVA through swelling and thermal analyses, *Proc. 16th Brazilian Polym. Conf.*, 2021, 24–28.

75 J. Choi, K. Min, Y. H. Mo, S. B. Han and T. H. Kim, Understanding the Effect of Triazole on Crosslinked PPO–SEBS-Based Anion Exchange Membranes for Water Electrolysis, *Polymers*, 2023, **15**, 1736, DOI: **10.3390/polym15071736**.

76 M. Sabzi, M. J. Afshari, M. Babaahmadi and N. Shafagh, pH-dependent swelling and antibiotic release from citric acid crosslinked poly(vinyl alcohol) (PVA)/nano silver hydrogels, *Colloids Surfaces B Biointerfaces*, 2020, **188**, 110757, DOI: **10.1016/j.colsurfb.2019.110757**.

77 M. Arshad, A. Neelam, N. Haleem, Y. Jamal, K. Hina, M. Bilal, S. H. Shah, I. Hussain and Y. Zhang, Synthesis and characterization of cmc/pva/pvp composite microfiltration membrane, *Desalin. Water Treat.*, 2020, **203**, 70–79, DOI: **10.5004/dwt.2020.26227**.

78 A. L. Ahmad, N. M. Yusuf and B. S. Ooi, Preparation and modification of poly (vinyl) alcohol membrane: Effect of crosslinking time towards its morphology, *Desalination*, 2012, **287**, 35–40, DOI: **10.1016/j.desal.2011.12.003**.

79 M. Huang, Y. Hou, Y. Li, D. Wang and L. Zhang, High performances of dual network PVA hydrogel modified by PVP using borax as the structure-forming accelerator, *Des. Monomers Polym.*, 2017, **20**, 505–513, DOI: **10.1080/15685551.2017.1382433**.